

Coulomb drag by motion of a monolayer polar crystal through graphene nano-constriction

A. L. Chudnovskiy¹

¹*I. Institut für Theoretische Physik, Universität Hamburg, Notkestraße 9, D-22607 Hamburg, Germany*

We predict theoretically that the motion of a polar crystalline layer between two graphene planes exerts Coulomb drag on electrons in graphene, inducing a DC-drag current. The physical mechanism of this drag relies on the intervalley scattering of charge carriers in graphene by the time-dependent potential of the moving crystalline layer. The drag current exhibits a nonlinear Hall effect, which can be used for the experimental measurement of the Berry curvature. In turn, the drag of electrons in graphene exerts a back-action on the crystalline layer, which can be expressed in terms of increased dynamic viscosity.

Recent experiments have shown that confining water in nano-constrictions leads to an ordering phase transition, resulting in a lattice of water molecules and forming a two-dimensional ice crystal [1–4]. Due to the inherent dipole moment of a water molecule, this single-layer ice forms a polar crystal with a frozen pattern of dipoles. Under applied external pressure, the ice layer can move through constrictions. A recent example of such motion is demonstrated in experiments in Refs. [5, 6], where water flowed through a nanoconstriction of a single graphene layer’s width between graphene planes. The motion of the spatially ordered dipole moments of the ice layer generates a time- and space-periodic electric field acting on the electrons in the walls of the constriction. Notably, the spatial period of the electric field set by the lattice spacing of the polar crystal is comparable to the nearest neighbor distance in graphene. For instance, for the crystal of square ice, the lattice spacing is given by $a_0 \approx 2.8 \text{ \AA}$ [1], which is comparable to the nearest neighbor distance in graphene $a = 1.42 \text{ \AA}$ [7]. Consequently, the momentum transferred from the moving crystal to the electrons in graphene is close to the distance between the K and K' points in reciprocal space. This opens the possibility for Coulomb drag of electrons in graphene induced by the motion of the polar crystalline layer, facilitated by intervalley and/or umklapp scattering processes. The fundamental physical mechanism for this drag involves intervalley transitions of electrons induced by the external time-dependent potential created by the moving crystalline layer.

In this paper, we investigate the DC-drag current density in graphene induced by the motion of a crystalline layer. We uncover several distinct features of the DC-drag current that set it apart from conventional drag phenomena: (i) The drag current is proportional to the velocity of the crystalline layer. (ii) The direction of the drag current is determined by the orientation of the moving crystalline lattice with respect to the vector connecting the two K-points in graphene, rather than the direction of the crystalline layer’s velocity. (iii) The drag exhibits signatures of the nonlinear Hall effect, which allows its use for experimental measurement of the Berry curvature.

(iv) The drag sets in at a finite doping level that creates Fermi surfaces around the K points. (v) Unlike conventional Coulomb or phonon drag, the leading contribution to the drag current is temperature-independent.

The scattering mechanism underlying the drag effect is similar to the umklapp scattering that causes excess resistivity in graphene/hexagonal boron nitride heterostructures [8]. However, unlike the stationary superlattice in heterostructures, scattering by the moving crystalline layer transfers energy to electrons in graphene, thereby inducing a finite drag current. The drag effect considered here also bears some analogy to the acousto-electric effect, where electric current is generated by acoustic waves [9–14]. The main difference lies in the very small wavelength associated with the potential of the moving polar crystal, which can induce intervalley transitions or umklapp processes. Although motivated by recent experiments on the ice layer sliding through the mammoconstriction, the drag phenomenon is of a quite general nature and is applicable to any two-dimensional (2D) polar crystal layer (see Fig. 1a).

Let us introduce the model for the Coulomb drag by a moving polar crystalline layer. The crystalline layer exerts a periodic potential on electrons in the immediate vicinity determined by its crystal structure, given by $U(\mathbf{r}) \sim \sum_{i=1,2} \cos(\mathbf{Q}_i \mathbf{r})$, where $\mathbf{Q}_{1,2}$ denote the reciprocal lattice vectors of the crystal. The potential of the moving crystal gains time dependence through a boost transformation $\mathbf{r} \rightarrow \mathbf{r} - \mathbf{v}_0 t$, where \mathbf{v}_0 denotes the velocity of the crystalline layer. Therefore, we model the periodic time-dependent potential exerted by the layer moving with velocity v_0 by the expression $U(\mathbf{r}, \mathbf{t}) = \sum_{i=1,2} U_i \cos(\mathbf{Q}_i(\mathbf{r} - \mathbf{v}_0 t))$. The scalar products of the vectors $\mathbf{Q}_{1,2}$ with the velocity of the crystalline layer determine the frequencies of the time dependent potential $\omega_i = (\mathbf{Q}_i \cdot \mathbf{v}_0)$. As will be shown below, the amplitude of the drag current is proportional to the frequency of the driving potential, hence the component of the potential with the higher frequency provides the dominant contribution to the drag. For instance, among several possible orderings of water molecules, the simplest one is a square ice, in which molecules are ordered in a one-layer square

lattice. In this configuration the vectors \mathbf{Q}_1 and \mathbf{Q}_2 are orthogonal. The maximal drag is achieved when one reciprocal wave vector, \mathbf{Q}_1 , is aligned with the velocity of the layer \mathbf{v}_0 . In this case, the other wave vector \mathbf{Q}_2 is perpendicular to the velocity, and its component provides no contribution to the drag. Therefore, in what follows we consider only one component of the periodic potential and drop the subscript at the wave vector \mathbf{Q} .

The external potential of the crystalline layer affects both the on-site energies and the nearest-neighbor hopping amplitudes in the graphene lattice. In this paper, we focus on the effect on the on-site energies. Modulation of the nearest-neighbor hopping does not lead to qualitatively new results, so we relegate its discussion to the Supplemental Material [15]. We describe the modulation of the on-site energies by the Hamiltonian

$$H_U = U_0 \sum_{n,m} \left\{ \cos(\mathbf{Q}\mathbf{r}_{nm} - \omega t) \bar{\psi}_A(\mathbf{r}_{nm}) \psi_A(\mathbf{r}_{nm}) + \cos(\mathbf{Q}(\mathbf{r}_{nm} + \boldsymbol{\delta}_3) - \omega t) \bar{\psi}_B(\mathbf{r}_{nm} + \boldsymbol{\delta}_3) \psi_B(\mathbf{r}_{nm} + \boldsymbol{\delta}_3) \right\}. \quad (1)$$

Here A and B denote the two sublattices of the hexagonal graphene lattice [7, 16]. The atoms of the A -sublattice are situated at $\mathbf{r}_{nm} = n\mathbf{a}_1 + m\mathbf{a}_2$, where n, m are integers and $\mathbf{a}_{1,2}$ denote the lattice vectors in graphene. The positions of atoms of the B -sublattice are given by $\mathbf{r}_{nm} + \boldsymbol{\delta}_3$ (see Fig. 1b).

Consider now the action of external potential Eqs. (1) as a source of the intervalley and umklapp scattering. An elementary scattering process requires conservation of energy and quasi-momentum (with $\hbar = 1$ throughout this paper)

$$\epsilon(\mathbf{p}) = \epsilon(\mathbf{p}') + \omega, \quad \mathbf{p}' + \mathbf{Q} = \mathbf{p} + n_1\mathbf{b}_1 + n_2\mathbf{b}_2 + m(\mathbf{K} - \mathbf{K}'). \quad (2)$$

Here n_1, n_2 , and m are integers, \mathbf{b}_1 and \mathbf{b}_2 denote the reciprocal lattice vectors in graphene, and \mathbf{K} and \mathbf{K}' denote the wave vectors at K -points. The wave vectors \mathbf{k}' and \mathbf{k} relate to the initial and the final states by the scattering event. The relation of wave-vectors for a scattering event with $n_1 = n_2 = 0, m = 1$ is shown in Fig. 1b). Using the data on the graphene lattice structure one can conclude that the minimal mismatch of the vectors \mathbf{k} and \mathbf{k}' is reached by the intervalley scattering, when the reciprocal lattice vector \mathbf{Q} of the crystalline layer is parallel to the vector $\mathbf{K} - \mathbf{K}'$ connecting the different K -points. Taking the length of the vector \mathbf{Q} proper to the square ice lattice, $|\mathbf{Q}| = 2\pi/a_0$, using the standard values for the K points

$$\mathbf{K} = \frac{2\pi}{3a}(1, 1/\sqrt{3}), \quad \mathbf{K}' = \frac{2\pi}{3a}(1, -1/\sqrt{3}), \quad (3)$$

and considering the geometry $\mathbf{Q} \parallel \mathbf{K} - \mathbf{K}' \parallel \hat{\mathbf{y}}$, we estimate the difference of the final and initial wave-vectors as

$$\mathbf{q} = \mathbf{p} - \mathbf{p}' = \mathbf{Q} - (\mathbf{K} - \mathbf{K}') \approx \frac{0.77}{a} \hat{\mathbf{y}}. \quad (4)$$

Absorption of the momentum \mathbf{q} by the electron system of graphene results in the drag current. Furthermore, energy conservation by scattering requires that the vector \mathbf{q} connects two states in the graphene energy band, that is $\epsilon(\mathbf{p} + \mathbf{q}) = \epsilon(\mathbf{p}) + \omega$. The maximal possible value of the frequency ω is given by $\omega = v_0|\mathbf{Q}|$. However, since the drift velocity of the ice layer $v_0 \sim 1$ m/s is much smaller than the electron velocity in graphene $v_F \sim 10^6$ m/s, the energy of the transition between the states with \mathbf{p} parallel to $\mathbf{p} + \mathbf{q}$, given by $v_F|\mathbf{q}|$, is much larger than ω . The energy conservation condition can be satisfied though, if the wave-vectors of the initial and final states are anti-parallel, lying at opposite points of the Fermi-surface, as shown in Fig. 1c). Then the energy conservation reads $v_F(|q| - 2p_F) = v_0|\mathbf{Q}|$, and it can be satisfied at the Fermi wave vector $p_F = \frac{1}{2}(|q| - \frac{v_0}{v_F}|\mathbf{Q}|)$. This Fermi wave vector marks the threshold for the Fermi energy $\mu = v_F p_F$, at which the drag current starts. For larger Fermi wave vectors, the conservation of energy and quasi-momentum can also be satisfied at some angle between the vectors \mathbf{p} and \mathbf{q} , as shown in Fig. 1b). Therefore, the intervalley scattering provides the most efficient drag mechanism under the conditions where the velocity and one crystallographic axis of the moving crystalline layer are parallel to the $\mathbf{K} - \mathbf{K}'$ vector in graphene.

Reaching the threshold chemical potential for the drag requires substantial doping, which nevertheless lies within the reach of modern experiments. Using the values $v_F \sim 10^6$ m/s, $v_0 \sim 1$ m/s, and $|\mathbf{q}| \sim |\mathbf{K} - \mathbf{K}' - \mathbf{Q}| \sim 5.5 \cdot 10^9 \text{ m}^{-1}$ (see Eq. 4), we estimate the threshold chemical potential as $\mu \sim 0.6t \sim 2$ eV. It is noteworthy that the threshold chemical potential is still below the van Hove singularity at the M-point of graphene $E_{\text{vH}} \sim 3eV$, so considering separate K points remains valid. In light of recent progress in doping graphene up to and even above the M-point [17, 18], reaching the threshold doping for the drag looks quite feasible. We estimate the electron density around the threshold as $n_e \sim 10^{18} \text{ m}^{-2}$.

Now let us proceed with calculation of the induced drag current. For the states close to the K and K' points, the electron spectrum in the graphene layer given by a well-known Hamiltonian [7, 16]

$$H_g = -iv_F \int d^2\mathbf{r} \left[\Psi_1^\dagger(\mathbf{r}) \boldsymbol{\sigma} \cdot \nabla \Psi_1(\mathbf{r}) + \Psi_2^\dagger(\mathbf{r}) \boldsymbol{\sigma}^* \cdot \nabla \Psi_2(\mathbf{r}) \right], \quad (5)$$

where the indexes 1, 2 correspond to the K and K' points respectively, and $\Psi(\mathbf{k}) = (\psi_A(\mathbf{k}), \psi_B(\mathbf{k}))^T$ denotes a spinor in the pseudospin space. Because the electron spin does not play a role in the drag physics considered here, spin indexes are suppressed. The interaction with the moving crystalline layer is given by Eqs. (1). Upon projecting Eq. (1) on the states close to the K points, the

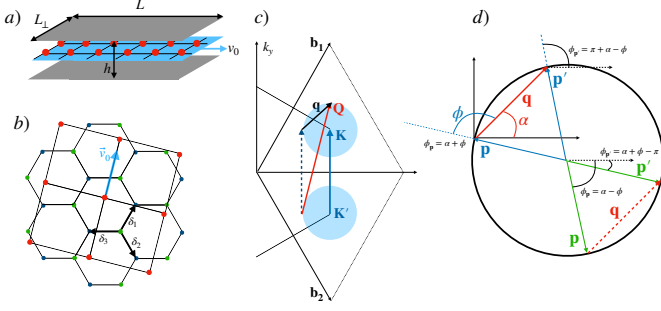


FIG. 1. a) Scheme of motion of a crystalline layer through a graphene nano-constriction. b) Graphene and square ice lattices. The maximal energy transfer $\omega = (\mathbf{v}_0 \cdot \mathbf{Q})$ is achieved when the velocity of the ice \mathbf{v}_0 is parallel to one of the main lattice directions (see the text). c) Reciprocal lattice of graphene. The vectors \mathbf{b}_1 , \mathbf{b}_2 indicate the first Brillouin zone. Filled circles denote the Fermi sea around the K and K' points. Arrows indicate the momentum conservation by intervalley transitions leading to the drag current $\mathbf{K} - \mathbf{K}' + \mathbf{q} = \mathbf{Q}$. d) Definitions of the angles α and ϕ and their relation to the directions of the initial (\mathbf{p}) and the final (\mathbf{p}') momenta by a single scattering event. At the threshold doping, the vector \mathbf{Q} is parallel to $\mathbf{K} - \mathbf{K}'$, the transferred quasi-momentum $\hbar\mathbf{q} = 2p_F$, the angle $\phi = \pm\pi$.

drag potential acquires the form

$$H_d = \frac{U_0}{2} \int_{\mathbf{p}} \left\{ \Psi_1^+(\mathbf{p} + \mathbf{q}) (\mathbf{u}(\mathbf{q}, \mathbf{p}) \cdot \boldsymbol{\sigma}) \Psi_2(\mathbf{p}) e^{-i\omega t} + \Psi_2^+(\mathbf{p}) (\mathbf{u}^*(\mathbf{q}, \mathbf{p}) \cdot \boldsymbol{\sigma}) \Psi_1(\mathbf{p} + \mathbf{q}) e^{i\omega t} \right\}, \quad (6)$$

where $(\mathbf{u}(\mathbf{q}, \mathbf{p}) \cdot \boldsymbol{\sigma}) = \sum_{i=0,3} u_i(\mathbf{q}, \mathbf{p}) \sigma_i$, and we set U_0 to be the energy scale characterizing the interaction strength. The interaction constants $u_{0,3}$ account for the shift of local on-site energies. We note in passing that modulation of the hopping amplitude introduces the terms $\sum_{i=1,2} u_i(\mathbf{q}, \mathbf{p}) \sigma_i$ with the constants $u_{1,2}$. Explicit form of the dimensionless coupling constants $u_i(\mathbf{q}, \mathbf{p})$ is provided in the Supplemental Material [15]. In writing Eq. (46) we retained only the time-dependent exponentials that can satisfy the energy conservation condition $v|\mathbf{p}| \pm \omega = v|\mathbf{p} \pm \mathbf{q}|$ according to the dispersion in graphene close to the K -points. We calculate the drag current in frame of perturbative expansion in the interaction strength U_0 using the Keldysh formalism. The unperturbed Green functions for the states near the K -points are determined by the Hamiltonian Eq. (5). They can be conveniently represented in the form that separates a valley independent pole structure and the valley dependent pseudospin structure $\hat{G}_\nu^{R/A}(\epsilon, \mathbf{p}) = G^{R/A}(\epsilon, \mathbf{p}) \hat{g}_\nu(\epsilon, \mathbf{p})$, where $G^{R/A}(\epsilon, \mathbf{p}) = \epsilon / [(\epsilon \pm \frac{i}{2\tau})^2 - v_F^2 p^2]$ denote the pseudospin-independent parts of the Green functions, and $\hat{g}_{K/K'}(\epsilon, \mathbf{p}) = \sigma_0 + \frac{v_F}{\epsilon} (p_x \sigma_x \pm p_y \sigma_y)$. Here the Pauli-matrices σ_i act on pseudospin. The Keldysh component of the Green functions is given by $\hat{G}_\nu^K(\epsilon, \mathbf{p}) =$

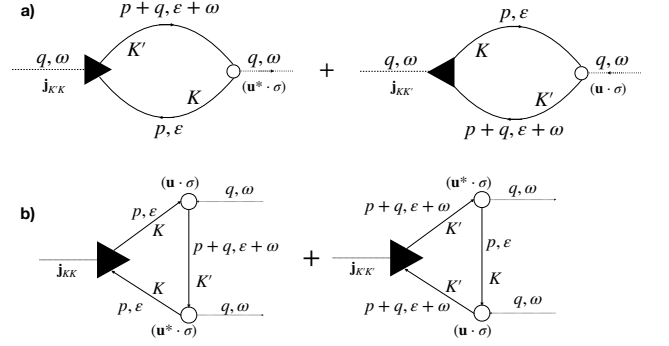


FIG. 2. Diagrams for the ac (panel a) and dc (panel b) drag current densities in the lowest order in interactions.

$\tanh\left(\frac{\epsilon}{2T}\right) \left(\hat{G}_\nu^R(\epsilon, \mathbf{p}) - \hat{G}_\nu^A(\epsilon, \mathbf{p}) \right)$. The lowest order contributions to the drag current density are given by the diagrams in Fig. (2), where solid lines denote Green functions for the states close to K and K' points. Detailed calculations of AC- and DC- drag current densities are provided in the Supplemental Material [15].

The AC drag current at the frequency ω is given by the diagrams of the first order in the interaction strength in Fig. 2a). Here the two diagrams correspond to the current induced in the K and K' valleys by intervalley scattering. However, we believe that the AC-drag will be strongly suppressed in the realistic experiment because of defects in the ice lattice structure. Those defects would lead to phase slips in the driving potential and eventually to a randomization of the phase, which in turn will suppress the AC drag current.

In contrast, the DC current is largely insensitive to small random changes in the phase of the driving potential. The total DC current density is calculated as a sum of contributions from the two valleys, $\mathbf{j}_{dc} = \langle \mathbf{j}_{KK} \rangle + \langle \mathbf{j}_{K'K'} \rangle$, each represented by a diagram in Fig. 2b). These diagrams depict the interaction-induced rectification, where the AC displacement current of the moving layer is converted into a DC drag current in graphene. Since the drag requires a finite chemical potential μ in graphene, the temperature effects are of minor importance for $T \ll \mu$, which is valid up to room temperature. In this case, the calculation of the diagrams in Fig. 2b) can be performed by setting $T = 0$. Furthermore, for $\mu > 0$ the states in conduction band provide the dominant contribution to the drag current. Upon projection on the states of conduction band, we obtain the following expression for the DC-drag current density

$$\mathbf{j}_{DC} = \frac{\pi^2 e U_0^2 p_F \omega \tau}{\hbar^3} \frac{\mathbf{F}^{DC}(\alpha, \phi)}{2v_F |q| |\sin \phi|} = \frac{\pi^4 v_0}{e \hbar a_0} \frac{U_0^2}{\rho_g v_F |q|} \frac{\mathbf{F}^{DC}(\alpha, \phi)}{|\sin \phi|}. \quad (7)$$

In the second equation, we express the mean free time τ through the resistivity of graphene $\rho_g = \frac{\pi \hbar}{e^2 \mu \tau}$, where $\mu = p_F v_F$ denotes the chemical potential. The DC-

drag is purely dissipative, with the drag current being proportional to the mean-free time τ of electron states in graphene. Additionally, we use the relation between the frequency and the velocity of the crystalline layer $\omega = 2\pi v_0/a_0$, assuming the velocity to be parallel to the vector $\mathbf{K} - \mathbf{K}'$ connecting the K-points in graphene.

The dependencies of the drag current on chemical potential for two different directions of the transferred quasi-momentum \mathbf{q} are shown in Fig. 3a). There is a sharp threshold chemical potential for the drag effect. Finite temperature leads to a smearing of the step at the threshold $\mu = \left(\frac{v_F|q|}{\omega} - 1\right)/2$, but it does not affect the qualitative dependence of the current on chemical potential. Above this threshold, the direction of the current is determined by the vector $\mathbf{F}^{\text{DC}}(\alpha, \phi)$, which is given by the product of matrix elements of the current density operator and interaction vertices $\mathbf{F}^{\text{DC}}(\alpha, \phi) = \Re[\mathbf{j}_{\mathbf{K}}(\mathbf{p})e^{i\phi_{\mathbf{p}}} - \mathbf{j}_{\mathbf{K}'}(\mathbf{p})e^{i\phi_{\mathbf{p}'}}]|\langle \mathbf{p} + \mathbf{q}, \mathbf{K}' | (\mathbf{u} \cdot \boldsymbol{\sigma}) | \mathbf{p}, \mathbf{K} \rangle|^2$, where $\phi_{\mathbf{p}} = \alpha \pm \phi$ denotes the direction of the vector \mathbf{p} , and $\phi_{\mathbf{p}'} = \alpha \mp \phi$ denotes the direction of the vector \mathbf{p}' , as shown in Fig. 1d). The angle α specifies the direction of the transferred quasi-momentum, and one might naively expect the drag current to align with this direction. This expectation holds true only when the reciprocal vector of the moving lattice is parallel to the vector connecting the K points in graphene, $\mathbf{Q} \parallel \mathbf{K}' - \mathbf{K}$. In the general case, the direction of the drag current deviates from the transferred quasi-momentum, as shown in Fig. 3b). This deviation is a signature of the nonlinear valley Hall effect. The nonlinear valley Hall effect bears an analogy with a nonlinear Hall effect considered previously in Refs. [19, 20]. It also suggests using the drag as a momentum-resolved probe of the Berry curvature $\Omega(\mathbf{p}, \mathbf{q})$. Specifically, the Berry curvature can be calculated from the relation of the longitudinal (with respect to transferred quasimomentum \mathbf{q}) j_q and Hall, j_H components of the drag current

$$\Omega(\mathbf{p}, \mathbf{q}) = \frac{\pi^2 j_H / j_q}{v_F q^2 \cos \phi} \Re \{ j_{q, \mathbf{K}}(\mathbf{p}) e^{i\phi_{\mathbf{p}}} + j_{q, \mathbf{K}'}(\mathbf{p} + \mathbf{q}) e^{i\phi_{\mathbf{p}+\mathbf{q}}} \} \quad (8)$$

Here the components of the drag current j_H , j_q are inferred from experimental measurements, whereas the matrix elements $j_{q, \mathbf{K}}(\mathbf{p})$, $j_{q, \mathbf{K}'}(\mathbf{p} + \mathbf{q})$ are known from theoretical calculations. Detailed derivation for Eq. (115) is provided in the Supplemental Material [15]. Fig. 3c) shows the Berry phase as a function of chemical potential. Changing the chemical potential, one probes the Berry curvature at different states at the Fermi surface, as shown at Fig. 1d).

The drag current given by Eq. (7) formally diverges at the threshold $p_F = \frac{1}{2}(q - \omega/v_F)$, corresponding to the angle $\phi = \pi$, as illustrated in the left panel in Fig. 3. That divergence is removed by accounting for scattering processes that change the momentum of quasiparticles. Considering the finite lifetime τ leads to the replacement $\sin \phi \rightarrow \frac{1}{\sqrt{v_F q \tau}}$ in Eq. (7) in the region $v_F |2p_F - q| < 1/\tau$

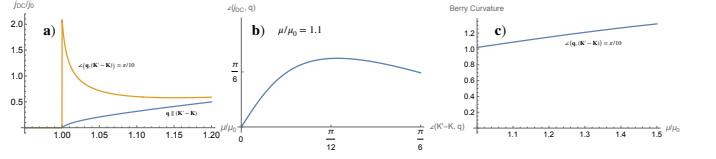


FIG. 3. a) DC drag current as function of chemical potential for two different directions of the transferred quasimomentum. The threshold chemical potential μ_0 corresponds to the transferred quasi-momentum $q = 2p_F$; b) The angle between the direction of the transferred quasimomentum $\mathbf{q} = \mathbf{Q} - (\mathbf{K}' - \mathbf{K})$ and the drag current \mathbf{j}_{DC} as function of the angle between \mathbf{q} and $\mathbf{K}' - \mathbf{K}$. In the absence of the Hall effect, the drag current would be parallel to \mathbf{q} ; c) Berry curvature as function of chemical potential.

close to the threshold. The vector-function $\mathbf{F}^{\text{DC}}(\alpha, \phi)$ remains nonsingular at the threshold value $\phi = \pi$.

Essentially, the drag effect considered here represents the conversion of the kinetic energy of the moving polar crystalline layer into the energy of a DC electric current in graphene. This energy transfer from the moving crystalline layer to the electrons in graphene results in the back-action force on the layer, which can be formulated in terms of a renormalized shear viscosity coefficient. If one adopts the Poiseuille equation for a crystalline layer moving with a velocity v between the two graphene layers, the following relation is obtained $\Delta p h L_{\perp} = 8\eta v L_{\perp} L/h$, where Δp denotes the pressure difference at the ends of the interlayer channel of the length L , h denotes the distance between the graphene layers forming the channel (see Fig. 1a), v is the velocity of the crystalline layer, and ν_0 denotes the shear viscosity in the absence of the drag current. To determine the change in shear viscosity due to the drag, consider the energy dissipation during the motion of the crystalline layer. In the absence of the drag current, the energy dissipation rate is given by the relation $\dot{Q}_0 = \Delta p h L_{\perp} v = 8\eta_0 v^2 L_{\perp} L/h$. The drag current results in the additional dissipation, given by $\dot{Q}_{\text{drag}} = 2j_d^2 L_{\perp}^2 \rho_g L = f_d^2 v^2 L_{\perp}^2 \rho_g L$, where $j_d = v f_d$ is the absolute value of the drag current density in graphene, ρ_g denotes the resistivity of the graphene layer, and the factor 2 accounts for the two layers forming the nano-channel. In the last equation, we took into account the proportionality of the drag current to the velocity of the moving layer, as given by Eq. (7). The coefficient f_d can be read from Eq. (7), $f_d = \frac{\pi^4}{e\hbar} \frac{U_0^2}{a_0 \rho_g v_F |q|} \frac{|\mathbf{F}^{\text{DC}}(\alpha, \phi)|}{|\sin \phi|}$. Therefore, the total energy dissipation in presence of the drag reads

$$\dot{Q}_0 + \dot{Q}_{\text{drag}} = \eta_0 v^2 \frac{8L_{\perp} L}{h} + f_d^2 v^2 L_{\perp}^2 \rho_g L \equiv \eta v^2 \frac{8L_{\perp} L}{h}, \quad (9)$$

where the last equation defines the renormalized shear friction coefficient η . Eq. (9) allows one to determine the shear friction coefficient due to the drag effect, $\eta = \eta_0 + \eta_d$, where $\eta_d = f_d^2 \rho_g L_{\perp} h/4$. The change in dynamic

viscosity provides an alternative way to detect the drag phenomenon. Specifically, crossing the drag threshold by altering the chemical potential of graphene would lead to a sharp decrease in the velocity of the crystalline layer, as described by the relation $\frac{v}{v_0} = \frac{\eta_0}{\eta_0 + \eta_d}$.

In summary, we predict a Coulomb drag effect that should be observable in experiments involving sliding polar crystalline layers through nano-constrictions between graphene planes. This drag mechanism hinges on the comparable lattice constants of graphene and the moving crystalline layer, which facilitates intervalley and umklapp scattering induced by the potential of the moving layer. The predicted effect can be experimentally detected through the induction of drag current or drag voltage in graphene planes, as well as by observing an increase in viscosity due to the motion of the crystalline layer, resulting in a reduction of its velocity. Moreover, the drag manifests a nonlinear intervalley Hall effect – specifically, a component of the drag current perpendicular to the transferred quasi-momentum. This effect can be used for a momentum-resolved determination of the Berry curvature. Achieving the drag effect requires significant doping of graphene to create sufficiently large Fermi surfaces around each K -point. Our estimations indicate that modern experimental doping levels are adequate for observing this phenomenon.

The author acknowledges fruitful discussions with M. Trushin, A. Kamenev, A. Levchenko, V. Cheianov, and T. Wehling.

-
- [1] G. Algara-Siller, O. Lehtinen, F. C. Wang, R. R. Nair, U. Kaiser, H. A. Wu, A. K. Geim, and I. V. Grigorieva, Square ice in graphene nanocapillaries, *Nature* **519**, 443 (2015).
- [2] S. Negi, A. Carvalho, M. Trushin, and A. H. C. Neto, Edge-driven phase transitions in 2d ice, *The Journal of Physical Chemistry C* **126**, 16006 (2022).
- [3] Z. Gao, N. Giovambattista, and O. Sahin, Phase diagram of water confined by graphene, *Scientific Reports* **8**, 6228 (2018).
- [4] S. Li and B. Schmidt, Two-dimensional water in graphene nanocapillaries simulated with different force fields: Rhombic versus square structures, proton ordering, and phase transitions (2019), [arXiv:1901.04236 \[physics.chem-ph\]](https://arxiv.org/abs/1901.04236).
- [5] K. Gopinadhan, S. Hu, A. Esfandiar, M. Lozada-Hidalgo, F. C. Wang, Q. Yang, A. V. Tyurnina, A. Keerthi, B. Radha, and A. K. Geim, Complete steric exclusion of ions and proton transport through confined monolayer water, *Science* **363**, 145 (2019).
- [6] R. R. Nair, H. A. Wu, P. N. Jayaram, I. V. Grigorieva, and A. K. Geim, Unimpeded permeation of water through helium-leak-tight graphene-based membranes, *Science* **335**, 442 (2012).
- [7] M. I. Katsnelson, *Graphene: Carbon in Two Dimensions* (Cambridge University Press, 2012).
- [8] J. R. Wallbank, R. Krishna Kumar, M. Holwill, Z. Wang, G. H. Auton, J. Birkbeck, A. Mishchenko, L. A. Ponomarenko, K. Watanabe, T. Taniguchi, K. S. Novoselov, I. L. Aleiner, A. K. Geim, and V. I. Fal’ko, Excess resistivity in graphene superlattices caused by umklapp electron–electron scattering, *Nature Physics* **15**, 32 (2019).
- [9] R. H. Parmenter, The acousto-electric effect, *Phys. Rev.* **89**, 990 (1953).
- [10] S. G. Eckstein, Acoustoelectric Effect, *Journal of Applied Physics* **35**, 2702 (1964).
- [11] A. Many and I. Balberg, The acoustoelectric effect, in *Electronic Structures in Solids: Lectures presented at the Second Chania Conference, held in Chania, Crete, June 30–July 14, 1968*, edited by E. D. Haidemenakis (Springer US, Boston, MA, 1969) pp. 385–416.
- [12] V. I. Fal’ko, S. V. Meshkov, and S. V. Iordanskii, Acoustoelectric drag effect in the two-dimensional electron gas at strong magnetic field, *Phys. Rev. B* **47**, 9910 (1993).
- [13] A. V. Kalameitsev, V. M. Kovalev, and I. G. Savenko, Valley acoustoelectric effect, *Phys. Rev. Lett.* **122**, 256801 (2019).
- [14] P. N. Lapa, G. Kassabian, F. Torres, P. Salev, M.-H. Lee, J. del Valle, and I. K. Schuller, Acoustoelectric drag current in vanadium oxide films, *Journal of Applied Physics* **128**, 155104 (2020).
- [15] A. L. Chudnovskiy, Supplemental material, Supplemental material.
- [16] A. H. Castro Neto, F. Guinea, N. M. R. Peres, K. S. Novoselov, and A. K. Geim, The electronic properties of graphene, *Rev. Mod. Phys.* **81**, 109 (2009).
- [17] P. Rosenzweig, H. Karakachian, S. Link, K. Küster, and U. Starke, Tuning the doping level of graphene in the vicinity of the van hove singularity via ytterbium intercalation, *Phys. Rev. B* **100**, 035445 (2019).
- [18] P. Rosenzweig, H. Karakachian, D. Marchenko, K. Küster, and U. Starke, Overdoping graphene beyond the van hove singularity, *Phys. Rev. Lett.* **125**, 176403 (2020).
- [19] E. Deyo, L. E. Golub, E. L. Ivchenko, and B. Spivak, *Semiclassical theory of the photogalvanic effect in non-centrosymmetric systems* (2009), [arXiv:0904.1917](https://arxiv.org/abs/0904.1917).
- [20] I. Sodemann and L. Fu, Quantum nonlinear hall effect induced by berry curvature dipole in time-reversal invariant materials, *Phys. Rev. Lett.* **115**, 216806 (2015).

**COULOMB DRAG BY MOTION OF A MONOLAYER POLAR CRYSTAL THROUGH GRAPHENE
NANO-CONSTRICTION: SUPPLEMENTAL MATERIAL**

In this Supplemental Material we provide detailed derivations of the formulas presented in the main text of the paper.

IMPORTANT LENGTH SCALES

Let us list the important length scales in graphene that will be used for further estimations. Lattice vectors in graphene:

$$\mathbf{a}_1 = \frac{a}{2}(3, \sqrt{3}), \quad \mathbf{a}_2 = \frac{a}{2}(3, -\sqrt{3}) \quad (10)$$

Vectors connecting the nearest neighbors atoms in graphene

$$\boldsymbol{\delta}_1 = \frac{a}{2}(1, \sqrt{3}), \quad \boldsymbol{\delta}_2 = \frac{a}{2}(1, -\sqrt{3}), \quad \boldsymbol{\delta}_3 = -a(1, 0). \quad (11)$$

$a \approx 1.42 \text{ \AA}$. Corresponding reciprocal-lattice vectors

$$\mathbf{b}_1 = \frac{2\pi}{3a}(1, \sqrt{3}), \quad \mathbf{b}_2 = \frac{2\pi}{3a}(1, -\sqrt{3}) \quad (12)$$

The K -points

$$\mathbf{K}' = \frac{2\pi}{3a}(1, 1/\sqrt{3}), \quad \mathbf{K} = \frac{2\pi}{3a}(1, -1/\sqrt{3}). \quad (13)$$

There are also equivalent K and K' points given by the vectors

$$\mathbf{K}' \Leftrightarrow \mathbf{K}' - \mathbf{b}_1 \Leftrightarrow \mathbf{K}' - \mathbf{b}_1 - \mathbf{b}_2, \quad \mathbf{K} \Leftrightarrow \mathbf{K} - \mathbf{b}_2 \Leftrightarrow \mathbf{K} - \mathbf{b}_1 - \mathbf{b}_2. \quad (14)$$

The lattice constant of the square ice crystal $a_0 \sim 2.8 \text{ \AA}$. Furthermore we put $\hbar = e = 1$ in all intermediate formulas.

OPERATOR OF ELECTRIC CURRENT DENSITY IN THE TIGHT-BINDING MODEL OF GRAPHENE

Since spin plays no role in further considerations, we suppress spin-indexes here and in what follows. The tight binding Hamiltonian of graphene (here the sublattices A, B correspond to pseudospin) is given by

$$H = it \sum_i \sum_{j=1}^3 (\psi_A^+(\mathbf{r}_i) \psi_B(\mathbf{r}_i + \boldsymbol{\delta}_j) - \psi_B^+(\mathbf{r}_i + \boldsymbol{\delta}_j) \psi_A(\mathbf{r}_i)) = \sum_{\mathbf{k}} (\psi_A^+(\mathbf{k}), \psi_B^+(\mathbf{k})) \begin{pmatrix} 0 & it \sum_{(j)} e^{i\mathbf{k}\boldsymbol{\delta}_j} \\ -it \sum_{(j)} e^{-i\mathbf{k}\boldsymbol{\delta}_j} & 0 \end{pmatrix} \begin{pmatrix} \psi_A(\mathbf{k}) \\ \psi_B(\mathbf{k}) \end{pmatrix}. \quad (15)$$

Here $\psi_{A,B}^+(\mathbf{r}_i), \psi_{A,B}(\mathbf{r}_i)$ denote fermion creation and annihilation operators at the site i of A and B sublattices respectively, and the sum over j runs over the nearest neighbor sites. External vector potential induces phase shifts on links $t_{ij} \rightarrow t_{ij} e^{i\phi_{ij}}$, where $\phi_{ij} = \mathbf{A}_i \cdot \boldsymbol{\delta}_j$ (the scalar product of the vector potential at the site i and the vector to the next-nearest neighbor j). In the (real-time) action, the coupling to the external vector potential is described by the following term

$$S_A = - \int_t \sum_i \sum_{j=1}^3 (\bar{\psi}_A(\mathbf{r}_i), \bar{\psi}_B(\mathbf{r}_i + \boldsymbol{\delta}_j)) \begin{pmatrix} 0 & ite^{i\phi_{ij}} \\ -ite^{-i\phi_{ij}} & 0 \end{pmatrix} \begin{pmatrix} \psi_A(\mathbf{r}_i) \\ \psi_B(\mathbf{r}_i + \boldsymbol{\delta}_j) \end{pmatrix}. \quad (16)$$

Transforming to the \mathbf{k} -space according to

$$\psi_A(\mathbf{r}) = \int_{\mathbf{k}} \psi_A(\mathbf{k}) e^{i\mathbf{k}\mathbf{r}}, \quad \psi_B(\mathbf{r} + \boldsymbol{\delta}_3) = \int_{\mathbf{k}} \psi_B(\mathbf{k}) e^{i\mathbf{k}\mathbf{r}}, \quad (17)$$

we obtain

$$S_A = - \int_t \sum_i \sum_{j=1}^3 \int_{\mathbf{k}, \mathbf{k}'} \left(\bar{\psi}_A(\mathbf{k}'), \bar{\psi}_B(\mathbf{k}') e^{-i\mathbf{k}'(\delta_j - \delta_3)} \right) e^{-i\mathbf{k}'\mathbf{r}_i} \begin{pmatrix} 0 & ite^{i\phi_{ij}} \\ -ite^{-i\phi_{ij}} & 0 \end{pmatrix} e^{i\mathbf{k}\mathbf{r}_i} \begin{pmatrix} \psi_A(\mathbf{k}) \\ \psi_B(\mathbf{k}) e^{i\mathbf{k}(\delta_j - \delta_3)} \end{pmatrix}. \quad (18)$$

The expression for the operator of the current density is obtained by the variation of the action with respect to the vector potential.

$$\mathbf{j}(\mathbf{r}_i) = \frac{\delta S}{\delta \mathbf{A}(\mathbf{r}_i)} = \sum_{\langle j \rangle} \delta_j \frac{\delta S}{\delta \phi_{ij}} \Big|_{\phi_{ij}=0} = \int_{\mathbf{k}, \mathbf{k}'} \sum_{j=1}^3 e^{i(\mathbf{k}-\mathbf{k}')\mathbf{r}_i} \left(\bar{\psi}_A(\mathbf{k}'), \bar{\psi}_B(\mathbf{k}') \right) \begin{pmatrix} 0 & -\delta_j t e^{i\mathbf{k}(\delta_j - \delta_3)} \\ -\delta_j t e^{-i\mathbf{k}'(\delta_j - \delta_3)} & 0 \end{pmatrix} \begin{pmatrix} \psi_A(\mathbf{k}) \\ \psi_B(\mathbf{k}) \end{pmatrix}. \quad (19)$$

Expansion of the current density operator for the states close to K and K' points.

Assume $\mathbf{k} = \mathbf{K} + \mathbf{p}$, $\mathbf{k}' = \mathbf{K}' + \mathbf{p}'$, ($|\mathbf{p}|, |\mathbf{p}'| \ll K, K'$). Then the current density operator can be represented as a sum of intra- and inter-valley components

$$\mathbf{j}(\mathbf{r}_i) = \mathbf{j}_{KK}(\mathbf{r}_i) + \mathbf{j}_{K'K'}(\mathbf{r}_i) + \mathbf{j}_{KK'}(\mathbf{r}_i) + \mathbf{j}_{K'K}(\mathbf{r}_i), \quad (20)$$

where for instance

$$\mathbf{j}_{K'K}(\mathbf{r}) = -t \sum_{j=1}^3 \int_{\mathbf{p}, \mathbf{p}'} e^{i(\mathbf{K}-\mathbf{K}'+\mathbf{p}-\mathbf{p}')\mathbf{r}} \left(\bar{\psi}_A(\mathbf{K}' + \mathbf{p}'), \bar{\psi}_B(\mathbf{K}' + \mathbf{p}') \right) \begin{pmatrix} 0 & \delta_j e^{i(\mathbf{K}+\mathbf{p})(\delta_j - \delta_3)} \\ \delta_j e^{-i(\mathbf{K}'+\mathbf{p}')(\delta_j - \delta_3)} & 0 \end{pmatrix} \begin{pmatrix} \psi_A(\mathbf{K} + \mathbf{p}) \\ \psi_B(\mathbf{K} + \mathbf{p}) \end{pmatrix}. \quad (21)$$

Let us introduce the pseudospin spinors for the states close to the K -points $\Psi_K(\mathbf{p}) = (\psi_A(\mathbf{K} + \mathbf{p}), \psi_B(\mathbf{K} + \mathbf{p}))$, $\Psi_{K'}(\mathbf{p}') = (\psi_A(\mathbf{K}' + \mathbf{p}'), \psi_B(\mathbf{K}' + \mathbf{p}'))$. Performing the Fourier transform and denoting $\mathbf{q} = \mathbf{p}' - \mathbf{p}$, we can write the Fourier component at the vector $\mathbf{K} - \mathbf{K}' - \mathbf{q}$ as

$$\mathbf{j}_{K'K}(\mathbf{q}) = \int_{\mathbf{p}} \bar{\Psi}_{K'}(\mathbf{p} + \mathbf{q}) \begin{pmatrix} 0 & -t \sum_{\langle j \rangle} \delta_j e^{i(\mathbf{K}+\mathbf{p})(\delta_j - \delta_3)} \\ -t \sum_{\langle j \rangle} \delta_j e^{-i(\mathbf{K}'+\mathbf{p}+\mathbf{q})(\delta_j - \delta_3)} & 0 \end{pmatrix} \Psi_K(\mathbf{p})$$

Let us introduce the operators of partial current density in each valley, which are defined as follows

$$\mathbf{j}_K(\mathbf{p}) = -t \sum_{j=1}^3 \delta_j e^{i(\mathbf{K}+\mathbf{p})(\delta_j - \delta_3)}, \quad \mathbf{j}_{K'}(\mathbf{p}) = -t \sum_{\langle j \rangle} \delta_j e^{i(\mathbf{K}'+\mathbf{p})(\delta_j - \delta_3)}. \quad (22)$$

Then the inter- and intra-valley components of the current density operator can be cast to the form

$$\mathbf{j}_{ab}(\mathbf{q}) = \int_{\mathbf{p}} (\bar{\Psi}_a(\mathbf{p} + \mathbf{q}) \mathbf{J}_{ab}(\mathbf{p}, \mathbf{p} + \mathbf{q}) \Psi_b(\mathbf{p})), \quad (23)$$

where

$$\mathbf{J}_{ab}(\mathbf{p} + \mathbf{q}, \mathbf{p}) = \begin{pmatrix} 0 & \mathbf{j}_b(\mathbf{p}) \\ \mathbf{j}_a^*(\mathbf{p} + \mathbf{q}) & 0 \end{pmatrix}. \quad (24)$$

Here the subscripts a, b relate to the valley, taking the values K, K' .

GREEN FUNCTIONS NEAR K POINTS IN THE KELDYSH FORMALISM

The Hamiltonian of graphene for the states close to the K, K' -points ($\mathbf{K} = \frac{2\pi}{3a}(1, -1/\sqrt{3})$, $\mathbf{K}' = \frac{2\pi}{3a}(1, 1/\sqrt{3})$) reads

$$H_K = v_F \int_{\mathbf{p}} \Psi_K^+(\mathbf{p})(\sigma_x p_x + \sigma_y p_y) \Psi_K(\mathbf{p}), \quad (25)$$

$$H_{K'} = v_F \int_{\mathbf{p}} \Psi_{K'}^+(\mathbf{p})(\mathbf{p})(\sigma_x p_x - \sigma_y p_y) \Psi_{K'}(\mathbf{p}), \quad (26)$$

where $v_F = \frac{3}{2}ta$ is the Fermi velocity. The Green functions in the Keldysh formalism have a matrix structure given by

$$\hat{G}(\epsilon, \mathbf{p}) = \begin{pmatrix} G^R(\epsilon, \mathbf{p}) & G^K(\epsilon, \mathbf{p}) \\ 0 & G^A(\epsilon, \mathbf{p}) \end{pmatrix}. \quad (27)$$

Here the superscripts $R/A/K$ relate to the retarded, advanced, and Keldysh components of the Green function respectively. According to the Hamiltonian Eq. (25), close to the K -point, the explicit form of the Green functions in equilibrium at temperature T is given by

$$G_K^{R/A}(\epsilon, \mathbf{p}) = \frac{\epsilon \mathbf{1}_2 + v_F \mathbf{p} \cdot \boldsymbol{\sigma}}{\epsilon^2 - v_F^2 p^2 \pm i0} = \frac{1}{\epsilon^2 - v_F^2 p^2 \pm i0} \begin{pmatrix} \epsilon & v_F(p_x - ip_y) \\ v_F(p_x + ip_y) & \epsilon \end{pmatrix} \quad (28)$$

$$G_K^K(\epsilon, \mathbf{p}) = \tanh\left(\frac{\epsilon}{2T}\right) (G^R(\epsilon, \mathbf{p}) - G^A(\epsilon, \mathbf{p})). \quad (29)$$

In what follows we introduce complexified momentum $p = p_x + ip_y$, denoting $\bar{p} = p_x - ip_y$, and $|p| = \sqrt{p_x^2 + p_y^2}$. Then the expressions for the Green functions can be represented in the form that exhibits their pole structure explicitly

$$G_K^{R/A}(\epsilon, \mathbf{p}) = \frac{1}{2} \left[\frac{1}{\epsilon - v_F |p| \pm i0} + \frac{1}{\epsilon + v_F |p| \pm i0} \right] \begin{pmatrix} 1 & v_F \bar{p}/\epsilon \\ v_F p/\epsilon & 1 \end{pmatrix}, \quad (30)$$

$$G_K^K(\epsilon, \mathbf{p}) = -i\pi \tanh\left(\frac{\epsilon}{2T}\right) \begin{pmatrix} 1 & v_F p/\epsilon \\ v_F \bar{p}/\epsilon & 1 \end{pmatrix} [\delta(\epsilon - v_F |p|) + \delta(\epsilon + v_F |p|)]. \quad (31)$$

The Green functions for momenta close to the K' point are determined by the Hamiltonian Eq. (26). They read

$$G_{K'}^{R/A}(\epsilon, \mathbf{p}) = \frac{\epsilon \mathbf{1}_2 + v_F \mathbf{p} \cdot \boldsymbol{\sigma}^*}{\epsilon^2 - v_F^2 p^2 \pm i0} = \frac{1}{\epsilon^2 - v_F^2 p^2 \pm i0} \begin{pmatrix} \epsilon & v_F(p_x + ip_y) \\ v_F(p_x - ip_y) & \epsilon \end{pmatrix}, \quad (32)$$

or, in the form explicitly exhibiting the pole structure,

$$G_{K'}^{R/A}(\epsilon, \mathbf{p}) = \frac{1}{2} \left[\frac{1}{\epsilon - v_F |p| \pm i0} + \frac{1}{\epsilon + v_F |p| \pm i0} \right] \begin{pmatrix} 1 & v_F p/\epsilon \\ v_F \bar{p}/\epsilon & 1 \end{pmatrix}, \quad (33)$$

$$G_{K'}^K(\epsilon, \mathbf{p}) = -i\pi \tanh\left(\frac{\epsilon}{2T}\right) \begin{pmatrix} 1 & v_F p/\epsilon \\ v_F \bar{p}/\epsilon & 1 \end{pmatrix} [\delta(\epsilon - v_F |p|) + \delta(\epsilon + v_F |p|)]. \quad (34)$$

Since the Green function in different valleys differ only by the matrix structure in the pseudospin space, it is convenient to introduce the following representation

$$\hat{G}_\nu^{R/A}(\epsilon, \mathbf{p}) = G^{R/A}(\epsilon, \mathbf{p}) \hat{g}_\nu(\epsilon, \mathbf{p}), \quad G_\nu^K(\epsilon, \mathbf{p}) = G^K(\epsilon, \mathbf{p}) \hat{g}_\nu(\epsilon, \mathbf{p}), \quad (35)$$

where

$$G^{R/A}(\epsilon, \mathbf{p}) = \frac{1}{2} \left[\frac{1}{\epsilon - v_F |p| \pm i0} + \frac{1}{\epsilon + v_F |p| \pm i0} \right], \quad (36)$$

$$G^K(\epsilon, \mathbf{p}) = -i\pi \tanh\left(\frac{\epsilon}{2T}\right) [\delta(\epsilon - v_F |p|) + \delta(\epsilon + v_F |p|)], \quad (37)$$

denote the parts of the Green functions independent of their pseudospin structure, and

$$\hat{g}_{K'}(\epsilon, \mathbf{p}) = \begin{pmatrix} 1 & v_F p/\epsilon \\ v_F \bar{p}/\epsilon & 1 \end{pmatrix} = \sigma_0 + \frac{v_F}{\epsilon} (p_x \sigma_x - p_y \sigma_y), \quad (38)$$

$$\hat{g}_K(\epsilon, \mathbf{p}) = \begin{pmatrix} 1 & v_F \bar{p}/\epsilon \\ v_F p/\epsilon & 1 \end{pmatrix} = \sigma_0 + \frac{v_F}{\epsilon} (p_x \sigma_x + p_y \sigma_y), \quad (39)$$

capture the structure of Green functions in the pseudospin space.

MODEL OF THE DRAG POTENTIAL BY MOVING POLAR CRYSTALLINE LAYER

In this section we provide detailed derivation of the interaction constants $u_i(\mathbf{q}, \mathbf{p})$ used in the main text of the paper. As it is explained in the main text, the dominant contribution to the drag is provided to the Fourier component of the crystalline potential that has a maximal projection upon the direction of velocity of the crystalline layer. In what follows we consider just that component, denoting its wave vector as \mathbf{Q} .

Modulation of on-site energies

We introduce the basis wave functions $\psi_{A,B}(\mathbf{r})$ localized at the positions of the atoms of the two (A, B) graphene sublattices. Thereby the atoms of the A -sublattice are situated at $\mathbf{r}_{nm} = n\mathbf{a}_1 + m\mathbf{a}_2$, where n, m are integers and $\mathbf{a}_{1,2}$ denote the lattice vectors in graphene, whereas the positions of atoms of the B -sublattice are given by $\mathbf{r}_{nm} + \boldsymbol{\delta}_3$. The action of the periodic potential on the on-site energies of the atoms is given by

$$H_U = U_0 \sum_{n,m} \left\{ \cos(\mathbf{Q}\mathbf{r}_{nm} - \omega t) \bar{\psi}_A(\mathbf{r}_{nm}) \psi_A(\mathbf{r}_{nm}) + \cos(\mathbf{Q}(\mathbf{r}_{nm} + \boldsymbol{\delta}_3) - \omega t) \bar{\psi}_B(\mathbf{r}_{nm} + \boldsymbol{\delta}_3) \psi_B(\mathbf{r}_{nm} + \boldsymbol{\delta}_3) \right\}$$

Performing Fourier-transform according to Eq. (17), we cast the external potential to the following expression

$$\begin{aligned} H_U = & \frac{U_0}{2} e^{-i\omega t} e^{\frac{i}{2}\mathbf{Q}\boldsymbol{\delta}_3} \int_{\mathbf{k}} \left\{ \cos\left(\frac{\mathbf{Q}}{2}\boldsymbol{\delta}_3\right) [\bar{\psi}_A(\mathbf{k} + \mathbf{Q})\psi_A(\mathbf{k}) + \bar{\psi}_B(\mathbf{k} + \mathbf{Q})\psi_B(\mathbf{k})] \right. \\ & \left. - i \sin\left(\frac{\mathbf{Q}}{2}\boldsymbol{\delta}_3\right) [\bar{\psi}_A(\mathbf{k} + \mathbf{Q})\psi_A(\mathbf{k}) - \bar{\psi}_B(\mathbf{k} + \mathbf{Q})\psi_B(\mathbf{k})] \right\} + \\ & e^{i\omega t} e^{-\frac{i}{2}\mathbf{Q}\boldsymbol{\delta}_3} \int_{\mathbf{k}} \left\{ \cos\left(\frac{\mathbf{Q}}{2}\boldsymbol{\delta}_3\right) [\bar{\psi}_A(\mathbf{k} - \mathbf{Q})\psi_A(\mathbf{k}) + \bar{\psi}_B(\mathbf{k} - \mathbf{Q})\psi_B(\mathbf{k})] \right. \\ & \left. + i \sin\left(\frac{\mathbf{Q}}{2}\boldsymbol{\delta}_3\right) [\bar{\psi}_A(\mathbf{k} - \mathbf{Q})\psi_A(\mathbf{k}) - \bar{\psi}_B(\mathbf{k} - \mathbf{Q})\psi_B(\mathbf{k})] \right\}. \end{aligned} \quad (40)$$

Frurthermore, using the pseudospin spinors $\Psi(\mathbf{k}) = (\psi_A(\mathbf{k}), \psi_B(\mathbf{k}))^T$, the Hamiltonian H_U can be written as

$$\begin{aligned} H_U = & \frac{U_0}{2} e^{-i\omega t} e^{\frac{i}{2}\mathbf{Q}\boldsymbol{\delta}_3} \int_{\mathbf{k}} \left\{ \cos\left(\frac{\mathbf{Q}}{2}\boldsymbol{\delta}_3\right) \bar{\Psi}(\mathbf{k} + \mathbf{Q})\sigma_0\Psi(\mathbf{k}) - i \sin\left(\frac{\mathbf{Q}}{2}\boldsymbol{\delta}_3\right) \bar{\Psi}(\mathbf{k} + \mathbf{Q})\sigma_z\Psi(\mathbf{k}) \right\} + \\ & e^{i\omega t} e^{-\frac{i}{2}\mathbf{Q}\boldsymbol{\delta}_3} \int_{\mathbf{k}} \left\{ \cos\left(\frac{\mathbf{Q}}{2}\boldsymbol{\delta}_3\right) \bar{\Psi}(\mathbf{k} - \mathbf{Q})\sigma_0\Psi(\mathbf{k}) + i \sin\left(\frac{\mathbf{Q}}{2}\boldsymbol{\delta}_3\right) \bar{\Psi}(\mathbf{k} - \mathbf{Q})\sigma_z\Psi(\mathbf{k}) \right\}, \end{aligned} \quad (41)$$

where $\sigma_0 = \mathbf{1}_2$ and σ_z denotes the Pauli matrix. Assuming \mathbf{Q} to be close to $\mathbf{K}' - \mathbf{K}$, we introduce the parametrization $\mathbf{Q} = \mathbf{K}' - \mathbf{K} + \mathbf{q}$. The external potential induces transitions between the electron states in different valleys. Then, assuming $|q| \ll |Q|$, we can represent Eq. (41) as

$$\begin{aligned} H_U = & \frac{U_0}{2} e^{-i\omega t} e^{\frac{i}{2}(\mathbf{K}' - \mathbf{K} + \mathbf{q})\boldsymbol{\delta}_3} \int_{\mathbf{p}} \left\{ \cos\left(\frac{\mathbf{K}' - \mathbf{K} + \mathbf{q}}{2}\boldsymbol{\delta}_3\right) \bar{\Psi}_{K'}(\mathbf{p} + \mathbf{q})\sigma_0\Psi_K(\mathbf{p}) - i \sin\left(\frac{\mathbf{K}' - \mathbf{K} + \mathbf{q}}{2}\boldsymbol{\delta}_3\right) \bar{\Psi}_{K'}(\mathbf{p} + \mathbf{q})\sigma_z\Psi_K(\mathbf{p}) \right\} \\ & + e^{i\omega t} e^{-\frac{i}{2}(\mathbf{K}' - \mathbf{K} + \mathbf{q})\boldsymbol{\delta}_3} \int_{\mathbf{p}} \left\{ \cos\left(\frac{\mathbf{K}' - \mathbf{K} + \mathbf{q}}{2}\boldsymbol{\delta}_3\right) \bar{\Psi}_K(\mathbf{p})\sigma_0\Psi_{K'}(\mathbf{p} + \mathbf{q}) + i \sin\left(\frac{\mathbf{K}' - \mathbf{K} + \mathbf{q}}{2}\boldsymbol{\delta}_3\right) \bar{\Psi}_K(\mathbf{p})\sigma_z\Psi_{K'}(\mathbf{p} + \mathbf{q}) \right\}, \end{aligned} \quad (42)$$

Further simplification is reached by noticing that $(\mathbf{K}' - \mathbf{K}) \cdot \boldsymbol{\delta}_3 = 0$, which results in

$$\begin{aligned} H_U = & \frac{U_0}{2} e^{-i\omega t} e^{\frac{i}{2}\mathbf{q}\boldsymbol{\delta}_3} \int_{\mathbf{p}} \left\{ \cos\left(\frac{\mathbf{q}}{2}\boldsymbol{\delta}_3\right) \bar{\Psi}_{K'}(\mathbf{p} + \mathbf{q})\sigma_0\Psi_K(\mathbf{p}) - i \sin\left(\frac{\mathbf{q}}{2}\boldsymbol{\delta}_3\right) \bar{\Psi}_{K'}(\mathbf{p} + \mathbf{q})\sigma_z\Psi_K(\mathbf{p}) \right\} + \\ & e^{i\omega t} e^{-\frac{i}{2}\mathbf{q}\boldsymbol{\delta}_3} \int_{\mathbf{p}} \left\{ \cos\left(\frac{\mathbf{q}}{2}\boldsymbol{\delta}_3\right) \bar{\Psi}_K(\mathbf{p})\sigma_0\Psi_{K'}(\mathbf{p} + \mathbf{q}) + i \sin\left(\frac{\mathbf{q}}{2}\boldsymbol{\delta}_3\right) \bar{\Psi}_K(\mathbf{p})\sigma_z\Psi_{K'}(\mathbf{p} + \mathbf{q}) \right\}. \end{aligned} \quad (43)$$

Change of the hopping amplitude by the potential of the moving lattice

We assume that the change of the hopping amplitude between the nearest neighbor atoms is proportional to the local external potential in the middle of the link connecting the two atoms in the graphene lattice. This assumption

leads to the following Hamiltonian for the change of the nearest-neighbor hopping

$$H_h = U_1 \sum_{\delta_1, \delta_2, \delta_3} \sum_{n, m} \left\{ \cos \left[\mathbf{Q} \left(\mathbf{r}_{nm} + \frac{\boldsymbol{\delta}_\nu}{2} \right) - \omega t \right] [\bar{\psi}_A(\mathbf{r}_{nm}) \psi_B(\mathbf{r}_{nm} + \boldsymbol{\delta}_\nu) + \bar{\psi}_B(\mathbf{r}_{nm} + \boldsymbol{\delta}_\nu) \psi_A(\mathbf{r}_{nm})] \right\} \quad (44)$$

Here the coupling constant U_1 is in general different from the coupling U_0 that describes the change of the local on-site potential. Performing the Fourier transformation in Eq. (44) into the \mathbf{k} space and leaving only the states close to K and K' point, we cast the Fourier transformed Hamiltonian H_h to the form

$$\begin{aligned} H_h = & \frac{U_1}{2} \sum_{i=1}^3 \int_{\mathbf{p}} \left\{ e^{-i\omega t} e^{\frac{i}{2} \boldsymbol{\delta}_3 (\mathbf{K}' - \mathbf{K} + \mathbf{q})} \bar{\Psi}_{K'}(\mathbf{q} + \mathbf{p}) \left(\sigma_x \cos \left[\left(\frac{\mathbf{K} + \mathbf{K}' + \mathbf{q}}{2} + \mathbf{p} \right) (\boldsymbol{\delta}_i - \boldsymbol{\delta}_3) \right] - \right. \right. \\ & \left. \left. \sigma_y \sin \left[\left(\frac{\mathbf{K} + \mathbf{K}' + \mathbf{q}}{2} + \mathbf{p} \right) (\boldsymbol{\delta}_i - \boldsymbol{\delta}_3) \right] \right) \Psi_K(\mathbf{p}) + \right. \\ & \left. e^{i\omega t} e^{-\frac{i}{2} \boldsymbol{\delta}_3 (\mathbf{K}' - \mathbf{K} + \mathbf{q})} \bar{\Psi}_K(\mathbf{p}) \left(\sigma_x \cos \left[\left(\frac{\mathbf{K} + \mathbf{K}' + \mathbf{q}}{2} + \mathbf{p} \right) (\boldsymbol{\delta}_i - \boldsymbol{\delta}_3) \right] - \right. \right. \\ & \left. \left. \sigma_y \sin \left[\left(\frac{\mathbf{K} + \mathbf{K}' + \mathbf{q}}{2} + \mathbf{p} \right) (\boldsymbol{\delta}_i - \boldsymbol{\delta}_3) \right] \right) \Psi_{K'}(\mathbf{p} + \mathbf{q}) \right\}. \end{aligned} \quad (45)$$

Total drag Hamiltonian

Upon projecting on the states close to the K points, the drag potential acquires the form

$$H_d = \frac{U_0}{2} \int_{\mathbf{p}} \left\{ \Psi_{K'}^+(\mathbf{p} + \mathbf{q}) (\mathbf{u}(\mathbf{q}, \mathbf{p}) \cdot \boldsymbol{\sigma}) \Psi_K(\mathbf{p}) e^{-i\omega t} + \Psi_K^+(\mathbf{p}) (\mathbf{u}^*(\mathbf{q}, \mathbf{p}) \cdot \boldsymbol{\sigma}) \Psi_{K'}(\mathbf{p} + \mathbf{q}) e^{i\omega t} \right\}, \quad (46)$$

where $(\mathbf{u}(\mathbf{q}) \cdot \boldsymbol{\sigma}) = \sum_{i=0}^3 u_i(\mathbf{q}) \sigma_i$. The components of the vector of coupling constants \mathbf{u} are obtained by comparison with Eqs. (43), (45) as follows

$$u_0 = \frac{1}{2} e^{\frac{i}{2} \mathbf{q} \boldsymbol{\delta}_3} \cos \left(\frac{\mathbf{q}}{2} \boldsymbol{\delta}_3 \right), \quad (47)$$

$$u_3 = -i \frac{1}{2} e^{\frac{i}{2} \mathbf{q} \boldsymbol{\delta}_3} \sin \left(\frac{\mathbf{q}}{2} \boldsymbol{\delta}_3 \right), \quad (48)$$

$$u_1 = \frac{U_1}{2U_0} e^{\frac{i}{2} \mathbf{q} \boldsymbol{\delta}_3} \sum_{i=1}^3 \cos \left[\left(\frac{\mathbf{K} + \mathbf{K}' + \mathbf{q}}{2} + \mathbf{p} \right) (\boldsymbol{\delta}_i - \boldsymbol{\delta}_3) \right] = \frac{U_1}{2U_0} e^{\frac{i}{2} \mathbf{q} \boldsymbol{\delta}_3} \left(1 - \sum_{i=1}^2 \cos \left[\left(\frac{\mathbf{q}}{2} + \mathbf{p} \right) (\boldsymbol{\delta}_i - \boldsymbol{\delta}_3) \right] \right), \quad (49)$$

$$u_2 = -\frac{U_1}{2U_0} e^{\frac{i}{2} \mathbf{q} \boldsymbol{\delta}_3} \sum_{i=1}^3 \sin \left[\left(\frac{\mathbf{K} + \mathbf{K}' + \mathbf{q}}{2} + \mathbf{p} \right) (\boldsymbol{\delta}_i - \boldsymbol{\delta}_3) \right] = \frac{U_1}{2U_0} e^{\frac{i}{2} \mathbf{q} \boldsymbol{\delta}_3} \sum_{i=1}^2 \sin \left[\left(\frac{\mathbf{q}}{2} + \mathbf{p} \right) (\boldsymbol{\delta}_i - \boldsymbol{\delta}_3) \right], \quad (50)$$

where in the second equalities we took into account $\frac{\mathbf{K} + \mathbf{K}'}{2} \cdot (\boldsymbol{\delta}_1 - \boldsymbol{\delta}_3) = \frac{\mathbf{K} + \mathbf{K}'}{2} \cdot (\boldsymbol{\delta}_2 - \boldsymbol{\delta}_3) = \pi$. Here we use the coupling U_0 as the overall scale for the coupling strengths.

PROJECTION ON THE CONDUCTION BAND

Due to the necessity of finite doping, the main contribution to the drag current at low temperature is produced by transitions between the quantum states in the conduction band. This observation allows simplified calculation of the current by projection on the conduction band. To realize the projection, we first employ the unitary rotation that diagonalizes the Hamiltonian in the pseudospin sector. Let ϕ_p be the polar angle of the wave vector $\mathbf{p} = (p_x, p_y)$. Then the Hamiltonian of the state with the wave vector \mathbf{p} is diagonalized by the unitary transformation

$$H(\mathbf{p}) = \begin{pmatrix} v_F |p| & 0 \\ 0 & -v_F |p| \end{pmatrix} = U_\nu^+(\phi_p) H_\nu(\mathbf{p}) U_\nu(\phi_p), \quad (51)$$

where

$$U_K(\mathbf{p}) = \frac{1}{\sqrt{2}} \begin{pmatrix} e^{-i\phi_p/2} & e^{-i\phi_p/2} \\ e^{i\phi_p/2} & -e^{i\phi_p/2} \end{pmatrix}, \quad U_{K'}(\mathbf{p}) = \frac{1}{\sqrt{2}} \begin{pmatrix} e^{i\phi_p/2} & e^{i\phi_p/2} \\ e^{-i\phi_p/2} & -e^{-i\phi_p/2} \end{pmatrix} \quad (52)$$

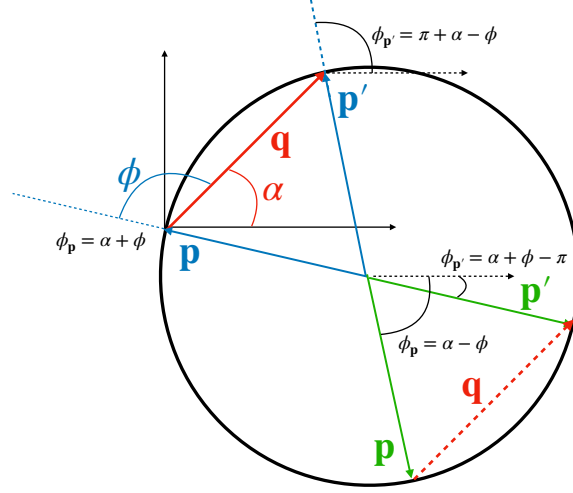


FIG. 4. Possible directions of initial and finite wave vectors for a given transfer wave vector \mathbf{q}

Further projection on the conduction band is achieved by the application of the operator $\frac{1}{2}(1 + \sigma_z)$, so that the total projection operator reads

$$\hat{P}_\nu^c(\mathbf{p}) = U_\nu(\mathbf{p}) \begin{pmatrix} 1 & 0 \\ 0 & 0 \end{pmatrix} \quad (53)$$

Explicitly, close to the points K and K' , the eigenstates of the conduction band are expressed through the eigenstates of A and B sublattices as follows

$$|p\rangle_c^K = \frac{1}{\sqrt{2}} \left(e^{-i\phi_{\mathbf{p}}/2} |A\rangle + e^{i\phi_{\mathbf{p}}/2} |B\rangle \right), \quad |p\rangle_c^{K'} = \frac{1}{\sqrt{2}} \left(e^{i\phi_{\mathbf{p}}/2} |A\rangle + e^{-i\phi_{\mathbf{p}}/2} |B\rangle \right) \quad (54)$$

Let us now consider the kinematic restriction on the wave vectors of the initial and final states due to the energy and quasi-momentum conservation in detail. Since the energy transfer by the scattering processes considered here is much smaller than the Fermi energy, we can approximately set the absolute value of the wave vectors for the initial and final states equal to the Fermi wave vector p_F . It turns out that this condition leaves only two possible choices for the wave vector of the initial state \mathbf{p} (the wave vector of the final state is then fixed automatically to $\mathbf{p} + \mathbf{q}$) for the fixed transferred wave vector \mathbf{q} (see Fig. 4). Denote the polar angle of the wave vector \mathbf{q} as α and the angle between vectors \mathbf{q} and \mathbf{p} as ϕ . Then the two possible choices are

$$\text{i) } \phi_{\mathbf{p}} = \alpha + \phi, \quad \phi_{\mathbf{p}'} = \pi + \alpha - \phi, \quad (55)$$

$$\text{ii) } \phi_{\mathbf{p}} = \alpha - \phi, \quad \phi_{\mathbf{p}'} = \alpha + \phi - \pi \Leftrightarrow \pi + \alpha + \phi. \quad (56)$$

It follows that all results for the case (ii) are obtained from (i) by change $\phi \rightarrow -\phi$. The change of the sign of the transfer quasi-momentum $\mathbf{q} \rightarrow -\mathbf{q}$ corresponds to the change $\alpha \rightarrow \alpha + \pi$.

Let us write down explicit expression for the components of current density operators Eqs. (22) projected on the conduction band. We consider the geometry as given in the case (i) above.

$$\mathbf{j}_K(\mathbf{p}) = -ta \left\{ \begin{pmatrix} -1 \\ 0 \end{pmatrix} + \begin{pmatrix} 1/2 \\ \sqrt{3}/2 \end{pmatrix} e^{i\frac{2\pi}{3}} e^{i\sqrt{3}ap_F \cos(\alpha + \phi - \pi/6)} + \begin{pmatrix} 1/2 \\ -\sqrt{3}/2 \end{pmatrix} e^{-i\frac{2\pi}{3}} e^{i\sqrt{3}ap_F \cos(\alpha + \phi + \pi/6)} \right\} \quad (57)$$

$$\mathbf{j}_{K'}(\mathbf{p} + \mathbf{q}) = \mathbf{j}_{K'}(\mathbf{p}') = -ta \left\{ \begin{pmatrix} -1 \\ 0 \end{pmatrix} + \begin{pmatrix} 1/2 \\ \sqrt{3}/2 \end{pmatrix} e^{-i\frac{2\pi}{3}} e^{-i\sqrt{3}ap_F \cos(\alpha - \phi - \pi/6)} + \begin{pmatrix} 1/2 \\ -\sqrt{3}/2 \end{pmatrix} e^{i\frac{2\pi}{3}} e^{-i\sqrt{3}ap_F \cos(\alpha - \phi + \pi/6)} \right\} \quad (58)$$

The projection of the current density operator on the conduction band is calculated using Eqs. (57), (58) as follows

$$\begin{aligned} \langle \mathbf{p} + \mathbf{q}, K' | \mathbf{j}_{K'K}(\mathbf{p} + \mathbf{q}, \mathbf{p}) | \mathbf{p}, K \rangle_c &= \frac{1}{2} \left(e^{-i\phi'/2}, e^{i\phi'/2} \right) \begin{pmatrix} 0 & \mathbf{j}_K(\mathbf{p}) \\ \mathbf{j}_{K'}^*(\mathbf{p} + \mathbf{q}) & 0 \end{pmatrix} \begin{pmatrix} e^{-i\phi/2} \\ e^{i\phi/2} \end{pmatrix} = \\ &= \frac{1}{2} \left\{ \mathbf{j}_K(\mathbf{p}) e^{i(\phi - \phi')/2} + \mathbf{j}_{K'}^*(\mathbf{p} + \mathbf{q}) e^{-i(\phi - \phi')/2} \right\}, \end{aligned} \quad (59)$$

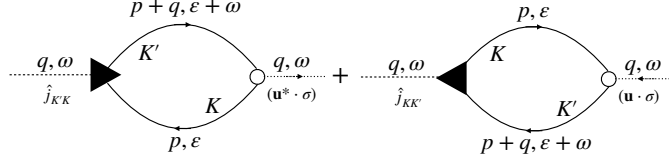


FIG. 5. Diagram for the lowest order contribution to the AC current.

$$\begin{aligned} \langle \mathbf{p}, K | \mathbf{J}_{KK'}(\mathbf{p}, \mathbf{p} + \mathbf{q}) | \mathbf{p} + \mathbf{q}, K' \rangle_c &= \langle \mathbf{p} + \mathbf{q}, K' | \mathbf{J}_{K'K}(\mathbf{p} + \mathbf{q}, \mathbf{p}) | \mathbf{p}, K \rangle_c^* = \\ &= \frac{1}{2} \left\{ \mathbf{j}_{K'}^*(\mathbf{p}) e^{-i(\phi - \phi')/2} + \mathbf{j}_{K'}(\mathbf{p} + \mathbf{q}) e^{i(\phi - \phi')/2} \right\}, \end{aligned} \quad (60)$$

where $\phi = \phi_{\mathbf{p}}$ and $\phi' = \phi_{\mathbf{p}'}$ as defined by Eqs. (55), (56).

For further calculations we also need the expressions for the projected interaction vertices

$$\langle \mathbf{p} + \mathbf{q}, K' | u_0 \sigma_0 | \mathbf{p}, K \rangle_c = -\frac{1}{2} e^{-\frac{i}{2}|q|a \cos \alpha} \cos \left(\frac{|q|a}{2} \cos \alpha \right) \sin \alpha, \quad (61)$$

$$\langle \mathbf{p} + \mathbf{q}, K' | u_3 \sigma_z | \mathbf{p}, K \rangle_c = \frac{1}{2} e^{-\frac{i}{2}|q|a \cos \alpha} \sin \left(\frac{|q|a}{2} \cos \alpha \right) \cos \alpha, \quad (62)$$

$$\langle \mathbf{p} + \mathbf{q}, K' | u_1 \sigma_x | \mathbf{p}, K \rangle_c = \frac{U_1}{2U_0} e^{-\frac{i}{2}|q|a \cos \alpha} \sin \phi \left\{ 1 - \cos \left[p_F a \sin \phi \cos \left(\frac{\pi}{3} - \alpha \right) \right] - \cos \left[p_F a \sin \phi \cos \left(\frac{2\pi}{3} - \alpha \right) \right] \right\}, \quad (63)$$

$$\langle \mathbf{p} + \mathbf{q}, K' | u_2 \sigma_y | \mathbf{p}, K \rangle_c = -\frac{U_1}{2U_0} e^{-\frac{i}{2}|q|a \cos \alpha} \cos \phi \left\{ \sin \left[p_F a \sin \phi \cos \left(\frac{\pi}{3} - \alpha \right) \right] + \sin \left[p_F a \sin \phi \cos \left(\frac{2\pi}{3} - \alpha \right) \right] \right\}. \quad (64)$$

PERTURBATIVE CALCULATION OF THE AC DRAG CURRENT

The diagram in Fig. 5 corresponds to the lowest order contribution to the current density due to the intervalley scattering (KK'). The mathematical expression reads

$$\langle J_{K'K}(\mathbf{q}, \omega) \rangle = -iU_0 \text{Tr} \left\{ \gamma^q \mathbf{J}_{K'K}(\mathbf{p} + \mathbf{q}, \mathbf{p}) \hat{G}_K(\mathbf{p}, \epsilon) (\mathbf{u}^*(\mathbf{q}, \mathbf{p}) \cdot \boldsymbol{\sigma}) \gamma^{\text{cl}} \hat{G}_{K'}(\mathbf{p} + \mathbf{q}, \epsilon + \omega) \right\}. \quad (65)$$

Here $\gamma^q = \sigma_1$ and $\gamma^{\text{cl}} = \sigma_0$ denote the Pauli matrices acting in the Keldysh (RA) space.

Using the notations introduced in Eq. (35), we separate the parts reflecting the pole structure of Green functions (the spectrum) and the part corresponding to the matrix elements of the transition in the pseudo-spin and valley spaces

$$\begin{aligned} \langle J_{K'K}(\mathbf{q}, \omega) \rangle &= -iU_0 \int_{\epsilon, \mathbf{p}} I_{K'K} \left\{ G^K(\mathbf{p}, \epsilon) G^A(\mathbf{p} + \mathbf{q}, \epsilon + \omega) + G^R(\mathbf{p}, \epsilon) G^K(\mathbf{p} + \mathbf{q}, \epsilon + \omega) \right\} = \\ &= -iU_0 \int_{\epsilon, \mathbf{p}} I_{K'K} \left\{ \tanh \left(\frac{\epsilon - \mu}{2T} \right) \left[G^R(\mathbf{p}, \epsilon) - G^A(\mathbf{p}, \epsilon) \right] G^A(\mathbf{p} + \mathbf{q}, \epsilon + \omega) + \right. \\ &= G^R(\mathbf{p}, \epsilon) \left[G^R(\mathbf{p} + \mathbf{q}, \epsilon + \omega) - G^A(\mathbf{p} + \mathbf{q}, \epsilon + \omega) \right] \tanh \left(\frac{\epsilon + \omega - \mu}{2T} \right) \left. \right\} = \\ &= -iU_0 \int_{\epsilon, \mathbf{p}} I_{K'K} \left\{ \left[\tanh \left(\frac{\epsilon - \mu}{2T} \right) - \tanh \left(\frac{\epsilon + \omega - \mu}{2T} \right) \right] G^R(\mathbf{p}, \epsilon) G^A(\mathbf{p} + \mathbf{q}, \epsilon + \omega) \right\}, \end{aligned} \quad (66)$$

where in the last line we omitted the products of two retarded and two advanced Green functions, and introduced the notation

$$I_{K'K}(\epsilon, \mathbf{p}; \omega, \mathbf{q}) = \text{tr} \left\{ \mathbf{J}_{K'K}(\mathbf{p}, \mathbf{p} + \mathbf{q}) g_K(\mathbf{p}, \epsilon) (\mathbf{u}^*(\mathbf{q}, \mathbf{p}) \cdot \boldsymbol{\sigma}) g_{K'}(\mathbf{p} + \mathbf{q}, \epsilon + \omega) \right\} \quad (67)$$

Analogously, the contribution to the current by the scattering from the valley K' to the valley K is given by

$$\langle J_{KK'}(\mathbf{q}, \omega) \rangle = -iU_0 \int_{\epsilon, \mathbf{p}} I_{KK'} \left\{ \left[\tanh \left(\frac{\epsilon + \omega - \mu}{2T} \right) - \tanh \left(\frac{\epsilon - \mu}{2T} \right) \right] G^R(\mathbf{p} + \mathbf{q}, \epsilon + \omega) G^A(\mathbf{p}, \epsilon) \right\}, \quad (68)$$

where

$$I_{KK'}(\epsilon, \mathbf{p}; \omega, \mathbf{q}) = \text{tr} \{ \mathbf{J}_{KK'}(\mathbf{p}, \mathbf{p} + \mathbf{q}) g_{K'}(\mathbf{p} + \mathbf{q}, \epsilon + \omega) (\mathbf{u}(\mathbf{q}, \mathbf{p}) \cdot \boldsymbol{\sigma}) g_K(\mathbf{p}, \epsilon) \}. \quad (69)$$

Momentum and frequency integration

Closing the integration contour in the lower ϵ half-plane, we reduce the integral to the sum over the residue of the poles of the retarded Green function, which results in

$$\begin{aligned} \langle J_{K'K}(\mathbf{q}, \omega) \rangle &= \frac{-\pi U_0}{2} \int_{\epsilon, \mathbf{p}} I_{K'K} \left[\tanh \left(\frac{\epsilon + \omega - \mu}{2T} \right) - \tanh \left(\frac{\epsilon - \mu}{2T} \right) \right] \times \\ &\left\{ \delta(\epsilon - v_F |p|) \left[\frac{1}{\omega + v_F |p| - v_F |p + q| - i/\tau} + \frac{1}{\omega + v_F |p| + v_F |p + q| - i/\tau} \right] + \right. \\ &\left. \delta(\epsilon + v_F |p|) \left[\frac{1}{\omega - v_F |p| - v_F |p + q| - i/\tau} + \frac{1}{\omega - v_F |p| + v_F |p + q| - i/\tau} \right] \right\} \end{aligned} \quad (70)$$

$$\begin{aligned} \langle J_{KK'}(\mathbf{q}, \omega) \rangle &= \frac{-\pi U_0}{2} \int_{\epsilon, \mathbf{p}} I_{KK'} \left[\tanh \left(\frac{\epsilon + \omega - \mu}{2T} \right) - \tanh \left(\frac{\epsilon - \mu}{2T} \right) \right] \times \\ &\left\{ \delta(\epsilon + \omega - v_F |\mathbf{p} + \mathbf{q}|) \left[\frac{1}{-\omega + v_F |\mathbf{p} + \mathbf{q}| - v_F |p| - i/\tau} + \frac{1}{-\omega + v_F |\mathbf{p} + \mathbf{q}| + v_F |p| - i/\tau} \right] + \right. \\ &\left. \delta(\epsilon + \omega + v_F |\mathbf{p} + \mathbf{q}|) \left[\frac{1}{-\omega - v_F |\mathbf{p} + \mathbf{q}| - v_F |p| - i/\tau} + \frac{1}{-\omega - v_F |\mathbf{p} + \mathbf{q}| + v_F |p| - i/\tau} \right] \right\} \end{aligned} \quad (71)$$

Here we introduced small imaginary part at the poles $i0 \rightarrow \frac{i}{2\tau}$, which accounts phenomenologically for intrinsic scattering processes in graphene.

Furthermore, leaving only the pole contributions to the integrals over momentum \mathbf{p} , we obtain

$$\begin{aligned} \langle J_{K'K}(\mathbf{q}, \omega) \rangle &= \frac{i\pi^2 U_0}{2} \int_{\mathbf{p}} \left\{ I_{K'K}(\epsilon = v_F |p| - \omega) \left[\tanh \left(\frac{\omega + v_F |p| - \mu}{2T} \right) - \tanh \left(\frac{v_F |p| - \mu}{2T} \right) \right] \times \right. \\ &[\delta(\omega + v_F |p| - v_F |p + q|) + \delta(\omega + v_F |p| + v_F |p + q|)] + \\ &I_{K'K}(\epsilon = -v_F |p|) \left[\tanh \left(\frac{\omega - v_F |p| - \mu}{2T} \right) - \tanh \left(\frac{-v_F |p| - \mu}{2T} \right) \right] \times \\ &[\delta(\omega - v_F |p| - v_F |p + q|) + \delta(\omega - v_F |p| + v_F |p + q|)] \left. \right\} \approx \\ &\frac{i\pi^2 U_0}{2} \int_{\mathbf{p}} I_{K'K}(\epsilon = v_F |p|) \left[\tanh \left(\frac{\omega + v_F |p| - \mu}{2T} \right) - \tanh \left(\frac{v_F |p| - \mu}{2T} \right) \right] \delta(\omega + v_F |p| - v_F |p + q|), \end{aligned} \quad (72)$$

$$\begin{aligned} \langle J_{KK'}(\mathbf{q}, \omega) \rangle &= \frac{i\pi^2 U_0}{2} \int_{\mathbf{p}} \left\{ I_{KK'}(\epsilon = v_F |\mathbf{p} + \mathbf{q}| - \omega) \left[\tanh \left(\frac{v_F |\mathbf{p} + \mathbf{q}| - \mu}{2T} \right) - \tanh \left(\frac{v_F |\mathbf{p} + \mathbf{q}| - \omega - \mu}{2T} \right) \right] \times \right. \\ &[\delta(v_F |\mathbf{p} + \mathbf{q}| - \omega - v_F |p|) + \delta(-\omega + v_F |p| + v_F |\mathbf{p} + \mathbf{q}|)] + \\ &I_{KK'}(\epsilon = -\omega - v_F |\mathbf{p} + \mathbf{q}|) \left[\tanh \left(\frac{-v_F |\mathbf{p} + \mathbf{q}| - \mu}{2T} \right) - \tanh \left(\frac{-v_F |\mathbf{p} + \mathbf{q}| - \omega - \mu}{2T} \right) \right] \times \\ &[\delta(-\omega - v_F |\mathbf{p} + \mathbf{q}| - v_F |p|) + \delta(-\omega - v_F |\mathbf{p} + \mathbf{q}| + v_F |p|)] \left. \right\} \approx \\ &\frac{i\pi^2 U_0}{2} \int_{\mathbf{p}} I_{KK'}(\epsilon = v_F |p|) \left[\tanh \left(\frac{v_F |p| + \omega - \mu}{2T} \right) - \tanh \left(\frac{v_F |p| - \mu}{2T} \right) \right] \delta(v_F |\mathbf{p} + \mathbf{q}| - \omega - v_F |p|). \end{aligned} \quad (73)$$

In the last lines of Eqs. (72), (73) we left the leading contributions at positive chemical potential and low temperatures. The combination of tanh-functions in that term together with the energy and quasi-momentum conservation imposed by the δ -function projects the integrals on the states of conduction band.

It is convenient to perform the two-dimensional integration over momenta using polar coordinates, $p = (|\mathbf{p}|, \phi)$ where ϕ is defined as the angle between vectors \mathbf{p} and \mathbf{q} . Furthermore, we satisfy the δ -functions by performing the angular integration. The angular integrals are calculated according to the formula

$$\int d\phi \delta(f(\phi)) F(\phi) = \frac{F(\phi_0)}{|f'(\phi_0)|}, \quad (74)$$

where $f'(\phi_0) = \frac{df(\phi)}{d\phi}|_{\phi=\phi_0}$, and ϕ_0 satisfies the relation $f(\phi_0) = 0$. Here we show explicitly the computation of the integral with $\delta(\omega + v_F|p| - v_F|p+q|)$ in Eq. (72). The angular dependence in the δ -function is contained in the term

$$|p+q| = \sqrt{p^2 + q^2 + 2pq \cos \phi}, \quad (75)$$

therefore

$$f(\phi) = \omega + v_F p - v_F \sqrt{p^2 + q^2 + 2pq \cos \phi}, \quad f'(\phi) = \frac{v_F p q \sin \phi}{\sqrt{p^2 + q^2 + 2pq \cos \phi}} = \frac{v_F p q \sin \phi}{|p+q|} = \frac{v_F^2 p q \sin \phi}{\omega + v_F p}, \quad (76)$$

where in the last equation we used the condition imposed by the δ -function.

Furhermore, in the physically relevant regime $v_F p \gg \omega$, we can simplify

$$f'(\phi) \approx v_F q \sin \phi. \quad (77)$$

At low temperature, $T \ll \omega$, the tanh can be replaced by a step function. Then, the integration over the absolute value of momentum $|p|$ can be performed by replacing $|p| \approx p_F$, whereas the difference of the step-functions determines the integration range ω/v_F . Thus, the low-temperature approximation to the integration can be summarized by the expression

$$\int_{\mathbf{p}} \left[\tanh\left(\frac{\omega + v_F|p| - \mu}{2T}\right) - \tanh\left(\frac{v_F|p| - \mu}{2T}\right) \right] \delta(v_F|\mathbf{p} + \mathbf{q}| - \omega - v_F|p|) \dots \approx \frac{\omega p_F}{v_F^2 |q|} \int d|p| \int \frac{d\phi}{\sin \phi} \delta(|p| - p_F) \delta(\phi - \phi_0) \dots, \quad (78)$$

where ϕ_0 is the angle between \mathbf{p} and \mathbf{q} that solves the equation $|\mathbf{p} + \mathbf{q}| = |p| = p_F$, which is explicitly given by

$$\phi_0 = \arccos\left(-\frac{q}{2p_F}\right). \quad (79)$$

Finally, the AC drag current density, given by the sum of Eqs. (72) and (73) becomes

$$\begin{aligned} \mathbf{j}_{\text{AC}} &= \frac{i\pi^2 U_0}{2} \int_{\mathbf{p}} (I_{K'K}(|p|, \mathbf{q}, \phi) + I_{KK'}(|p|, \mathbf{q}, \phi)) \left[\tanh\left(\frac{\omega + v_F|p| - \mu}{2T}\right) - \tanh\left(\frac{v_F|p| - \mu}{2T}\right) \right] \delta(\omega + v_F|p| - v_F|p+q|) = \\ &= \frac{i\pi^2 U_0}{2v_F|q| \sin \phi_0} \int p dp (I_{K'K}(|p|, \mathbf{q}, \phi_0) + I_{KK'}(|p|, \mathbf{q}, \phi_0)) \left[\tanh\left(\frac{\omega + v_F|p| - \mu}{2T}\right) - \tanh\left(\frac{v_F|p| - \mu}{2T}\right) \right] \approx \\ &= \frac{i\pi^2 U_0}{2v_F|q| \sin \phi_0} \frac{p_F \omega}{v_F} (I_{K'K}(p_F, \mathbf{q}, \phi_0) + I_{KK'}(p_F, \mathbf{q}, \phi_0)) = \frac{i\pi^2 U_0 \omega p_F}{2v_F|q| \sin \phi_0} (\mathcal{I}_{K'K}(p_F, \mathbf{q}, \phi_0) + \mathcal{I}_{K'K}(p_F, \mathbf{q}, \phi_0)), \end{aligned} \quad (80)$$

where in the last line we introduced the dimensionless parital current densities \mathcal{I}_{ab} defined by the relation

$$I_{ab}(p_F, \mathbf{q}, \phi_0) = v_F \mathcal{I}_{ab}(p_F, \mathbf{q}, \phi_0). \quad (81)$$

The drag current given by Eq. (80) formally diverges at the threshold $p_F = \frac{1}{2}(q - \omega/v_F)$, which corresponds to the angle $\phi_0 = \pi$. That divergence is removed if one takes into account the scattering processes that change momentum of quasiparticles. Therefore, close to the threshold, one should take into account the finite life-time τ in Eqs. (70), (71) explicitly, which amounts to the replacement $\sin \phi_0 \rightarrow \frac{1}{\sqrt{v_F q \tau}}$ in Eq. (80) at the cutoff $\phi_0 = \pi$. The exact dependence of the prefactor in Eq. (80) on the angle ϕ exhibits a crossover from the constant $\sqrt{v_F q \tau}$ for the angles satisfying $\sin \phi \ll \frac{1}{\sqrt{v_F q \tau}}$ to $1/\sin \phi$ for $\sin \phi \gg \frac{1}{\sqrt{v_F q \tau}}$.

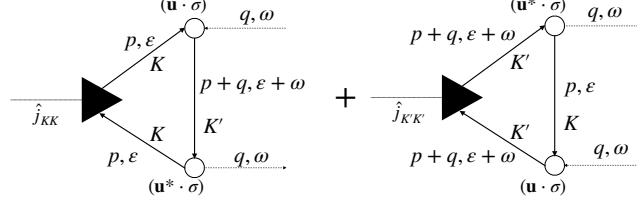


FIG. 6. Diagram for the lowest order contribution to the DC current.

Drag current density

In terms of the matrix elements projected onto the conduction band, the drag current density given by Eq. (80) can be cast in the form

$$\begin{aligned}
 \mathbf{j}_{AC} &\approx \frac{i\pi^2 U_0 \omega p_F}{2v_F |q| |\sin \phi|} \{ \langle \mathbf{p} + \mathbf{q}, K' | \mathbf{J}_{K'K}(\mathbf{p} + \mathbf{q}, \mathbf{p}) | K, \mathbf{p} \rangle \langle \mathbf{p}, K | \mathbf{u}^* \boldsymbol{\sigma} | \mathbf{p} + \mathbf{q}, K' \rangle + \\
 &\quad \langle \mathbf{p}, K | \mathbf{J}_{KK'}(\mathbf{p}, \mathbf{p} + \mathbf{q}) | K', \mathbf{p} + \mathbf{q} \rangle \langle \mathbf{p} + \mathbf{q}, K' | \mathbf{u} \boldsymbol{\sigma} | \mathbf{p}, K \rangle \} \\
 &= \frac{i\pi^2 U_0 \omega p_F}{2v_F |q| |\sin \phi|} \Re \left[\left(\mathbf{j}_K(\mathbf{p}) e^{i(\phi - \phi')/2} + \mathbf{j}_{K'}^*(\mathbf{p} + \mathbf{q}) e^{-i(\phi - \phi')/2} \right) \langle \mathbf{p}, K | \mathbf{u}^* \boldsymbol{\sigma} | \mathbf{p} + \mathbf{q}, K' \rangle \right] \\
 &= \frac{i\pi^2 U_0 \omega p_F}{2v_F |q| |\sin \phi|} \mathbf{F}_{K'K}^{AC}(\alpha, \phi) \tag{82}
 \end{aligned}$$

where the dimensionless vector function $\mathbf{F}_{K'K}^{AC}(\alpha, \phi)$ is determined by the matrix elements of the current density operator and interaction vertices. It depends only on the directions of the transferred quasi-momentum and the momenta of the initial and final scattered states, parametrized by the angles α, ϕ as shown in Fig. 4).

PERTURBATIVE CALCULATION OF THE DC DRAG CURRENT

The lowest order contributions to the current density of the DC drag are shown in Fig. 6. Here only the intra-valley current vertices contribute.

Calculation of the J_{KK} term

The first diagram (with the vertex j_{KK}) in Fig. 6 corresponds to the expression

$$\begin{aligned}
 \langle J_{KK}(\mathbf{q}, \omega) \rangle &= -iU_0^2 \text{Tr} \left\{ \gamma^q \mathbf{J}_{KK}(\mathbf{p}, \mathbf{p}) \hat{G}_K(\mathbf{p}, \epsilon) \gamma^{\text{cl}}(\mathbf{u}^*(\mathbf{q}, \mathbf{p}) \cdot \boldsymbol{\sigma}) \hat{G}_{K'}(\mathbf{p} + \mathbf{q}, \epsilon + \omega) \gamma^{\text{cl}}(\mathbf{u}(\mathbf{q}, \mathbf{p}) \cdot \boldsymbol{\sigma}) \hat{G}_K(\mathbf{p}, \epsilon) \right\} = \\
 &= -iU_0^2 \int_{\epsilon, \mathbf{p}} \text{Tr} \left\{ \mathbf{J}_{KK}(\mathbf{p}, \mathbf{p}) \left[G_K^K(\epsilon, \mathbf{p}) (\mathbf{u}^*(\mathbf{q}, \mathbf{p}) \cdot \boldsymbol{\sigma}) G_{K'}^A(\epsilon + \omega, \mathbf{p} + \mathbf{q}) (\mathbf{u}(\mathbf{q}, \mathbf{p}) \cdot \boldsymbol{\sigma}) G_K^A(\epsilon, \mathbf{p}) + \right. \right. \\
 &\quad G_K^R(\epsilon, \mathbf{p}) (\mathbf{u}^*(\mathbf{q}, \mathbf{p}) \cdot \boldsymbol{\sigma}) G_{K'}^K(\epsilon + \omega, \mathbf{p} + \mathbf{q}) (\mathbf{u}(\mathbf{q}, \mathbf{p}) \cdot \boldsymbol{\sigma}) G_K^A(\epsilon, \mathbf{p}) + \\
 &\quad \left. \left. G_K^R(\epsilon, \mathbf{p}) (\mathbf{u}^*(\mathbf{q}, \mathbf{p}) \cdot \boldsymbol{\sigma}) G_{K'}^R(\epsilon + \omega, \mathbf{p} + \mathbf{q}) (\mathbf{u}(\mathbf{q}, \mathbf{p}) \cdot \boldsymbol{\sigma}) G_K^K(\epsilon, \mathbf{p}) \right] \right\}. \tag{83}
 \end{aligned}$$

Using the notations Eq. (35), one can represent the expression for the current $\langle J_{KK} \rangle$ in the form

$$\begin{aligned}
 \langle J_{KK} \rangle &= -i \int_{\epsilon, \mathbf{p}} \left\{ G^R(\epsilon, \mathbf{p}) G^A(\epsilon, \mathbf{p}) \left[\tanh \left(\frac{\epsilon + \omega - \mu}{2T} \right) - \tanh \left(\frac{\epsilon - \mu}{2T} \right) \right] [G^R(\epsilon + \omega, \mathbf{p} + \mathbf{q}) - G^A(\epsilon + \omega, \mathbf{p} + \mathbf{q})] + \right. \\
 &\quad \left. \tanh \left(\frac{\epsilon - \mu}{2T} \right) \left[(G^R(\epsilon, \mathbf{p}))^2 G^R(\epsilon + \omega, \mathbf{p} + \mathbf{q}) - (G^A(\epsilon, \mathbf{p}))^2 G^A(\epsilon + \omega, \mathbf{p} + \mathbf{q}) \right] \right\} \times \\
 &\text{tr} \left\{ \mathbf{J}_{KK}(\mathbf{p}, \mathbf{p}) \hat{g}_K(\epsilon, \mathbf{p}) (\mathbf{u}^*(\mathbf{q}, \mathbf{p}) \cdot \boldsymbol{\sigma}) \hat{g}_{K'}(\epsilon + \omega, \mathbf{p} + \mathbf{q}) (\mathbf{u}(\mathbf{q}, \mathbf{p}) \cdot \boldsymbol{\sigma}) \hat{g}_K(\epsilon, \mathbf{p}) \right\}. \tag{84}
 \end{aligned}$$

In the following calculation we neglect the term in the second line in Eq. (84) that contains traces of three retarded or three advanced Green functions.

The trace in the pseudospin space leads to the sum of the terms proportional to combinations of different components of the driving potential,

$$\text{tr} \{ \mathbf{J}_{KK}(\mathbf{p}, \mathbf{p}) \hat{g}_K(\epsilon, \mathbf{p}) (\mathbf{u}^*(\mathbf{q}, \mathbf{p}) \cdot \boldsymbol{\sigma}) \hat{g}_{K'}(\epsilon + \omega, \mathbf{p} + \mathbf{q}) (\mathbf{u}(\mathbf{q}, \mathbf{p}) \cdot \boldsymbol{\sigma}) \hat{g}_K(\epsilon, \mathbf{p}) \} = \sum_{\mu, \nu=0}^3 u_\mu u_\nu^* \mathbf{J}_K^{\mu\nu}(\epsilon, \omega; \mathbf{p}, \mathbf{q}), \quad (85)$$

where

$$\mathbf{J}_K^{\mu\nu}(\epsilon, \omega; \mathbf{p}, \mathbf{q}) = \text{tr} \{ \mathbf{J}_{KK}(\mathbf{p}, \mathbf{p}) \hat{g}_K(\epsilon, \mathbf{p}) \sigma_\mu \hat{g}_{K'}(\epsilon + \omega, \mathbf{p} + \mathbf{q}) \sigma_\nu \hat{g}_K(\epsilon, \mathbf{p}) \} \quad (86)$$

Substituting explicit expressions for Green functions Eqs. (36), (37), we obtain

$$\begin{aligned} \langle J_{KK} \rangle &= -\frac{\pi U_0^2}{4} \int_{\epsilon, \mathbf{p}} \sum_{\mu, \nu=0}^3 u_\mu u_\nu^* \mathbf{J}_K^{\mu\nu}(\epsilon, \omega; \mathbf{p}, \mathbf{q}) \left[\tanh\left(\frac{\epsilon + \omega - \mu}{2T}\right) - \tanh\left(\frac{\epsilon - \mu}{2T}\right) \right] \times \\ &[\delta(\epsilon + \omega - v_F|p + q|) + \delta(\epsilon + \omega + v_F|p + q|)] \left[\frac{1}{\epsilon - v_F|p| + \frac{i}{2\tau}} + \frac{1}{\epsilon + v_F|p| + \frac{i}{2\tau}} \right] \left[\frac{1}{\epsilon - v_F|p| - \frac{i}{2\tau}} + \frac{1}{\epsilon + v_F|p| - \frac{i}{2\tau}} \right] \approx \\ &-\frac{\pi U_0^2}{4} \int_{\epsilon, \mathbf{p}} \sum_{\mu, \nu=0}^3 u_\mu u_\nu^* \mathbf{J}_K^{\mu\nu}(\epsilon, \omega; \mathbf{p}, \mathbf{q}) \left[\tanh\left(\frac{\epsilon + \omega - \mu}{2T}\right) - \tanh\left(\frac{\epsilon - \mu}{2T}\right) \right] [\delta(\epsilon + \omega - v_F|p + q|) + \delta(\epsilon + \omega + v_F|p + q|)] \times \\ &\left[\frac{1}{(\epsilon - v_F|p|)^2 + \frac{1}{4\tau^2}} + \frac{1}{(\epsilon + v_F|p|)^2 + \frac{1}{4\tau^2}} \right] \approx \\ &-\frac{\pi^2 \tau U_0^2}{2} \int_{\epsilon, \mathbf{p}} \sum_{\mu, \nu=0}^3 u_\mu u_\nu^* \mathbf{J}_K^{\mu\nu}(\epsilon, \omega; \mathbf{p}, \mathbf{q}) \left[\tanh\left(\frac{\epsilon + \omega - \mu}{2T}\right) - \tanh\left(\frac{\epsilon - \mu}{2T}\right) \right] \times \\ &[\delta(\epsilon + \omega - v_F|p + q|) + \delta(\epsilon + \omega + v_F|p + q|)] [\delta(\epsilon - v_F|p|) + \delta(\epsilon + v_F|p|)] \approx \\ &-\frac{\pi^2 \tau U_0^2}{2} \int_{\mathbf{p}} \sum_{\mu, \nu=0}^3 u_\mu u_\nu^* \mathbf{J}_K^{\mu\nu}(\epsilon = v_F|p|, \omega; \mathbf{p}, \mathbf{q}) \left[\tanh\left(\frac{v_F|p| + \omega - \mu}{2T}\right) - \tanh\left(\frac{v_F|p| - \mu}{2T}\right) \right] \delta(v_F|p| + \omega - v_F|p + q|) \\ &-\frac{\pi^2 \tau U_0^2}{2} \int_{\mathbf{p}} \sum_{\mu, \nu=0}^3 u_\mu u_\nu^* \mathbf{J}_K^{\mu\nu}(\epsilon = -v_F|p|, \omega; \mathbf{p}, \mathbf{q}) \left[\tanh\left(\frac{\omega - v_F|p| - \mu}{2T}\right) - \tanh\left(\frac{-v_F|p| - \mu}{2T}\right) \right] \delta(\omega - v_F|p| + v_F|p + q|) = \\ &-\frac{\pi^2 \tau U_0^2}{2} \int_{\mathbf{p}} \sum_{\mu, \nu=0}^3 u_\mu u_\nu^* \mathbf{J}_K^{\mu\nu}(\epsilon = v_F|p|, \omega; \mathbf{p}, \mathbf{q}) \left[\tanh\left(\frac{v_F|p| + \omega - \mu}{2T}\right) - \tanh\left(\frac{v_F|p| - \mu}{2T}\right) \right] \delta(v_F|p| + \omega - v_F|p + q|). \end{aligned} \quad (87)$$

Calculations in Eq. (87) are performed under the assumptions of a large mean-free time, $1/\tau \ll v_F p_F$, which allowed replacing the Lorentz-functions by δ -functions. Furthermore, some δ -functions are eliminated by the condition $\omega \ll v_F|p|$. In the last line we assumed positive frequency $\omega > 0$.

Again, as in the case of AC current, the restrictions imposed by the energy and momentum conservation together with Fermi-distributions amount to projection onto the states in the conduction band at low temperatures. It shows up mathematically in that the main contribution in Eq. (87) for $\mu > 0$ is provided by the term with the combination $\left[\tanh\left(\frac{v_F|p| + \omega - \mu}{2T}\right) - \tanh\left(\frac{v_F|p| - \mu}{2T}\right) \right] \delta(v_F|p + q| - v_F|p| - \omega)$.

Symmetries by change $K \leftrightarrow K'$

The following symmetries between the K and K' points emerge in frame of the rotating wave approximation for the drag potential

$$K \rightarrow K' \implies \omega \rightarrow -\omega, \quad q \rightarrow -\bar{q}, \quad p \rightarrow \bar{p}, \quad (88)$$

where we used complex valued vectors $p = p_x + ip_y$, $q = q_x + iq_y$, and \bar{p}, \bar{q} denote the complex conjugated vectors. For the angles α and ϕ , the transformation Eq. (88) implies

$$\alpha \rightarrow \pi - \alpha, \quad \phi \rightarrow \pi - \phi. \quad (89)$$

Calculation of the $J_{K'K'}$ term

The contribution of the diagram with $J_{K'K'}$ vertex is obtained from the one for J_{KK} employing the symmetries between the expressions for K and K' valleys $K \rightarrow K' \implies \omega \rightarrow -\omega$, $q \rightarrow -\bar{q}$, $p \rightarrow \bar{p}$. Below we repeat the main formulas applying the symmetries to the equations for J_{KK} .

$$\begin{aligned} \langle J_{K'K'}(\mathbf{q}, \omega) \rangle &= -iU_0^2 \text{Tr} \left\{ \gamma^q \mathbf{J}_{K'K'}(\mathbf{p}, \mathbf{p}) \hat{G}_{K'}(\mathbf{p}, \epsilon) \gamma^{\text{cl}}(\mathbf{u}(\mathbf{q}, \mathbf{p}) \cdot \boldsymbol{\sigma}) \hat{G}_K(\mathbf{p} - \mathbf{q}, \epsilon - \omega) \gamma^{\text{cl}}(\mathbf{u}^*(\mathbf{q}, \mathbf{p}) \cdot \boldsymbol{\sigma}) \hat{G}_{K'}(\mathbf{p}, \epsilon) \right\} = \\ &= -iU_0^2 \int_{\epsilon, \mathbf{p}} \text{Tr} \left\{ \mathbf{J}_{K'K'}(\mathbf{p}, \mathbf{p}) \left[G_{K'}^K(\epsilon, \mathbf{p})(\mathbf{u}(\mathbf{q}, \mathbf{p}) \cdot \boldsymbol{\sigma}) G_K^A(\epsilon - \omega, \mathbf{p} - \mathbf{q})(\mathbf{u}^*(\mathbf{q}, \mathbf{p}) \cdot \boldsymbol{\sigma}) G_{K'}^A(\epsilon, \mathbf{p}) + \right. \right. \\ &= G_{K'}^R(\epsilon, \mathbf{p})(\mathbf{u}(\mathbf{q}, \mathbf{p}) \cdot \boldsymbol{\sigma}) G_K^K(\epsilon - \omega, \mathbf{p} - \mathbf{q})(\mathbf{u}^*(\mathbf{q}, \mathbf{p}) \cdot \boldsymbol{\sigma}) G_{K'}^A(\epsilon, \mathbf{p}) + \\ &= \left. G_{K'}^R(\epsilon, \mathbf{p})(\mathbf{u}(\mathbf{q}, \mathbf{p}) \cdot \boldsymbol{\sigma}) G_K^R(\epsilon - \omega, \mathbf{p} - \mathbf{q})(\mathbf{u}^*(\mathbf{q}, \mathbf{p}) \cdot \boldsymbol{\sigma}) G_{K'}^K(\epsilon, \mathbf{p}) \right\}. \quad (90) \end{aligned}$$

Reproducing the calculational steps for the calculation in K -valley, we subsequently obtain

$$\begin{aligned} \langle J_{K'K'} \rangle &= -i \int_{\epsilon, \mathbf{p}} \left\{ G^R(\epsilon, \mathbf{p}) G^A(\epsilon, \mathbf{p}) \left[\tanh\left(\frac{\epsilon - \omega - \mu}{2T}\right) - \tanh\left(\frac{\epsilon - \mu}{2T}\right) \right] [G^R(\epsilon - \omega, \mathbf{p} - \mathbf{q}) - G^A(\epsilon - \omega, \mathbf{p} - \mathbf{q})] + \right. \\ &= \left. \tanh\left(\frac{\epsilon - \mu}{2T}\right) \left[(G^R(\epsilon, \mathbf{p}))^2 G^R(\epsilon - \omega, \mathbf{p} - \mathbf{q}) - (G^A(\epsilon, \mathbf{p}))^2 G^A(\epsilon - \omega, \mathbf{p} - \mathbf{q}) \right] \right\} \times \\ &= \text{tr} \left\{ \mathbf{J}_{K'K'}(\mathbf{p}, \mathbf{p}) \hat{g}_{K'}(\epsilon, \mathbf{p})(\mathbf{u}(\mathbf{q}, \mathbf{p}) \cdot \boldsymbol{\sigma}) \hat{g}_K(\epsilon - \omega, \mathbf{p} - \mathbf{q})(\mathbf{u}^*(\mathbf{q}, \mathbf{p}) \cdot \boldsymbol{\sigma}) \hat{g}_{K'}(\epsilon, \mathbf{p}) \right\}. \quad (91) \end{aligned}$$

$$\text{tr} \left\{ \mathbf{J}_{K'K'}(\mathbf{p}, \mathbf{p}) \hat{g}_{K'}(\epsilon, \mathbf{p})(\mathbf{u}(\mathbf{q}, \mathbf{p}) \cdot \boldsymbol{\sigma}) \hat{g}_K(\epsilon - \omega, \mathbf{p} - \mathbf{q})(\mathbf{u}^*(\mathbf{q}, \mathbf{p}) \cdot \boldsymbol{\sigma}) \hat{g}_{K'}(\epsilon, \mathbf{p}) \right\} = \sum_{\mu, \nu=0}^3 u_\mu^* u_\nu \mathbf{J}_{K'}^{\mu\nu}(\epsilon, \omega; \mathbf{p}, \mathbf{q}), \quad (92)$$

where

$$\mathbf{J}_{K'}^{\mu\nu}(\epsilon, \omega; \mathbf{p}, \mathbf{q}) = \text{tr} \left\{ \mathbf{J}_{K'K'}(\mathbf{p}, \mathbf{p}) \hat{g}_{K'}(\epsilon, \mathbf{p}) \sigma_\mu \hat{g}_K(\epsilon - \omega, \mathbf{p} - \mathbf{q}) \sigma_\nu \hat{g}_{K'}(\epsilon, \mathbf{p}) \right\} \quad (93)$$

Shifting the integration variables $\epsilon \rightarrow \epsilon + \omega$, $\mathbf{p} \rightarrow \mathbf{p} + \mathbf{q}$ and neglecting the products of three retarded and three advanced Green functions, we obtain

$$\begin{aligned}
\langle J_{K'K'} \rangle &= -i \int_{\epsilon, \mathbf{p}} \left\{ G^R(\epsilon + \omega, \mathbf{p} + \mathbf{q}) G^A(\epsilon + \omega, \mathbf{p} + \mathbf{q}) \left[\tanh\left(\frac{\epsilon - \mu}{2T}\right) - \tanh\left(\frac{\epsilon + \omega - \mu}{2T}\right) \right] [G^R(\epsilon, \mathbf{p}) - G^A(\epsilon, \mathbf{p})] \right\} \times \\
&\text{tr} \{ \mathbf{J}_{K'K'}(\mathbf{p} + \mathbf{q}, \mathbf{p} + \mathbf{q}) \hat{g}_{K'}(\epsilon + \omega, \mathbf{p} + \mathbf{q}) (\mathbf{u}(\mathbf{q}, \mathbf{p} + \mathbf{q}) \cdot \boldsymbol{\sigma}) \hat{g}_K(\epsilon, \mathbf{p}) (\mathbf{u}^*(\mathbf{q}, \mathbf{p} + \mathbf{q}) \cdot \boldsymbol{\sigma}) \hat{g}_{K'}(\epsilon, \mathbf{p} + \mathbf{q}) \} = \\
&-\frac{\pi U_0^2}{4} \int_{\epsilon, \mathbf{p}} \sum_{\mu, \nu=0}^3 u_\mu u_\nu^* \mathbf{J}_{K'}^{\mu\nu}(\epsilon + \omega, \omega; \mathbf{p} + \mathbf{q}, \mathbf{q}) \left[\tanh\left(\frac{\epsilon - \mu}{2T}\right) - \tanh\left(\frac{\epsilon + \omega - \mu}{2T}\right) \right] [\delta(\epsilon - v_F|p|) + \delta(\epsilon + v_F|p|)] \times \\
&\left[\frac{1}{\epsilon + \omega - v_F|\mathbf{p} + \mathbf{q}| + \frac{i}{2\tau}} + \frac{1}{\epsilon + \omega + v_F|\mathbf{p} + \mathbf{q}| + \frac{i}{2\tau}} \right] \left[\frac{1}{\epsilon + \omega - v_F|\mathbf{p} + \mathbf{q}| - \frac{i}{2\tau}} + \frac{1}{\epsilon + \omega + v_F|\mathbf{p} + \mathbf{q}| - \frac{i}{2\tau}} \right] \approx \\
&-\frac{\pi U_0^2}{4} \int_{\epsilon, \mathbf{p}} \sum_{\mu, \nu=0}^3 u_\mu u_\nu^* \mathbf{J}_{K'}^{\mu\nu}(\epsilon + \omega, \omega; \mathbf{p} + \mathbf{q}, \mathbf{q}) \left[\tanh\left(\frac{\epsilon - \mu}{2T}\right) - \tanh\left(\frac{\epsilon + \omega - \mu}{2T}\right) \right] [\delta(\epsilon - v_F|p|) + \delta(\epsilon + v_F|p|)] \times \\
&\left[\frac{1}{(\epsilon + \omega - v_F|\mathbf{p} + \mathbf{q}|)^2 + \frac{1}{4\tau^2}} + \frac{1}{(\epsilon + \omega + v_F|\mathbf{p} + \mathbf{q}|)^2 + \frac{1}{4\tau^2}} \right] \approx \\
&-\frac{\pi^2 \tau U_0^2}{2} \int_{\epsilon, \mathbf{p}} \sum_{\mu, \nu=0}^3 u_\mu u_\nu^* \mathbf{J}_{K'}^{\mu\nu}(\epsilon + \omega, \omega; \mathbf{p} + \mathbf{q}, \mathbf{q}) \left[\tanh\left(\frac{\epsilon - \mu}{2T}\right) - \tanh\left(\frac{\epsilon + \omega - \mu}{2T}\right) \right] [\delta(\epsilon - v_F|p|) + \delta(\epsilon + v_F|p|)] \times \\
&[\delta(\epsilon + \omega - v_F|\mathbf{p} + \mathbf{q}|) + \delta(\epsilon + \omega + v_F|\mathbf{p} + \mathbf{q}|)] \approx \\
&-\frac{\pi^2 \tau U_0^2}{2} \int_{\mathbf{p}} \sum_{\mu, \nu=0}^3 u_\mu u_\nu^* \mathbf{J}_{K'}^{\mu\nu}(v_F|p| + \omega, \omega; \mathbf{p} + \mathbf{q}, \mathbf{q}) \left[\tanh\left(\frac{v_F|p| - \mu}{2T}\right) - \tanh\left(\frac{v_F|p| + \omega - \mu}{2T}\right) \right] \delta(v_F|p| + \omega - v_F|\mathbf{p} + \mathbf{q}|) - \\
&\frac{\pi^2 \tau U_0^2}{2} \int_{\mathbf{p}} \sum_{\mu, \nu=0}^3 u_\mu u_\nu^* \mathbf{J}_{K'}^{\mu\nu}(-v_F|p| + \omega, \omega; \mathbf{p} + \mathbf{q}, \mathbf{q}) \left[\tanh\left(\frac{-v_F|p| - \mu}{2T}\right) - \tanh\left(\frac{-v_F|p| + \omega - \mu}{2T}\right) \right] \delta(\omega + v_F|\mathbf{p} + \mathbf{q}| - v_F|p|) = \\
&-\frac{\pi^2 \tau U_0^2}{2} \int_{\mathbf{p}} \sum_{\mu, \nu=0}^3 u_\mu u_\nu^* \mathbf{J}_{K'}^{\mu\nu}(v_F|p| + \omega, \omega; \mathbf{p} + \mathbf{q}, \mathbf{q}) \left[\tanh\left(\frac{v_F|p| - \mu}{2T}\right) - \tanh\left(\frac{v_F|p| + \omega - \mu}{2T}\right) \right] \delta(v_F|p| + \omega - v_F|\mathbf{p} + \mathbf{q}|)
\end{aligned} \tag{94}$$

Total DC drag current

The total DC drag current density, given by the sum of Eqs. (87) and (94), can be represented in the form

$$\begin{aligned}
\mathbf{j}^{\text{DC}} &= -\frac{\pi^2 \tau U_0^2}{2} \int_{\mathbf{p}} \sum_{\mu, \nu=0}^3 [u_\mu(\mathbf{p}, \mathbf{q}) u_\nu^*(\mathbf{p}, \mathbf{q}) \mathbf{J}_K^{\mu\nu}(\epsilon = v_F|p|, \omega; \mathbf{p}, \mathbf{q}) - u_\mu(\mathbf{p} + \mathbf{q}, \mathbf{q}) u_\nu^*(\mathbf{p} + \mathbf{q}, \mathbf{q}) \mathbf{J}_{K'}^{\mu\nu}(\epsilon = v_F|p| + \omega, \omega; \mathbf{p} + \mathbf{q}, \mathbf{q})] \times \\
&\left[\tanh\left(\frac{v_F|p| + \omega - \mu}{2T}\right) - \tanh\left(\frac{v_F|p| - \mu}{2T}\right) \right] \delta(v_F|p| + \omega - v_F|p + q|).
\end{aligned} \tag{95}$$

Projection on the conduction band

The matrix elements of the current density operators between the states in conduction band are given by

$$\begin{aligned}
\langle \mathbf{p}, K | \mathbf{J}_{KK}(\mathbf{p}, \mathbf{p}) | \mathbf{p}, K \rangle_c &= \frac{1}{2} \left(e^{i\phi/2}, e^{-i\phi/2} \right) \begin{pmatrix} 0 & \mathbf{j}_K(\mathbf{p}) \\ \mathbf{j}_K^*(\mathbf{p}) & 0 \end{pmatrix} \begin{pmatrix} e^{-i\phi/2} \\ e^{i\phi/2} \end{pmatrix} = \\
&\frac{1}{2} \{ \mathbf{j}_K(\mathbf{p}) e^{i\phi} + \mathbf{j}_K^*(\mathbf{p}) e^{-i\phi} \},
\end{aligned} \tag{96}$$

where $\phi = \phi_{\mathbf{p}}$. Analogously, for the valley K' we obtain

$$\begin{aligned} \langle \mathbf{p}', K' | \mathbf{J}_{K'K'}(\mathbf{p}', \mathbf{p}') | \mathbf{p}', K' \rangle_c &= \frac{1}{2} \left(e^{-i\phi'/2}, e^{i\phi'/2} \right) \begin{pmatrix} 0 & \mathbf{j}_{K'}(\mathbf{p}') \\ \mathbf{j}_{K'}^*(\mathbf{p}') & 0 \end{pmatrix} \begin{pmatrix} e^{i\phi'/2} \\ e^{-i\phi'/2} \end{pmatrix} = \\ & \frac{1}{2} \left\{ \mathbf{j}_{K'}(\mathbf{p}') e^{-i\phi'} + \mathbf{j}_{K'}^*(\mathbf{p}') e^{i\phi'} \right\}, \end{aligned} \quad (97)$$

where $\phi' = \phi_{\mathbf{p}+\mathbf{q}}$ as given by Eqs. (55), (56).

Upon projection on the conduction band, the leading contributions to the DC drag current density are given by

$$\begin{aligned} \langle J_{KK} \rangle &\approx \frac{\pi^2 \tau}{2} U_0^2 \int_{\mathbf{p}} \sum_{\mu, \nu=0}^3 u_\mu u_\nu \mathbf{J}_K^{\mu\nu}(\epsilon = v_F |p|, \omega; \mathbf{p}, \mathbf{q}) \left[\tanh \left(\frac{v_F |p| + \omega - \mu}{2T} \right) - \tanh \left(\frac{v_F |p| - \mu}{2T} \right) \right] \delta(v_F |p+q| - v_F |p| - \omega) \approx \\ & \frac{\pi^2 U_0^2 \tau \omega p_F}{v_F |q| |\sin \phi|} \langle \mathbf{p}, K | \mathbf{J}_{KK}(\mathbf{p}, \mathbf{p}) | \mathbf{p}, K \rangle_c \langle \mathbf{p}, K | (\mathbf{u}^* \cdot \boldsymbol{\sigma}) | \mathbf{p} + \mathbf{q}, K' \rangle_c \langle \mathbf{p} + \mathbf{q}, K' | (\mathbf{u} \cdot \boldsymbol{\sigma}) | \mathbf{p}, K \rangle_c, \\ \langle J_{K'K'} \rangle &\approx -\frac{\pi^2 \tau U_0^2}{2} \int_{\mathbf{p}} \sum_{\mu, \nu=0}^3 u_\mu u_\nu^* \mathbf{J}_{K'}^{\mu\nu}(v_F |p| + \omega, \omega; \mathbf{p} + \mathbf{q}, \mathbf{q}) \left[\tanh \left(\frac{v_F |p| - \mu}{2T} \right) - \tanh \left(\frac{v_F |p| + \omega - \mu}{2T} \right) \right] \delta(v_F |p| + \omega - v_F |\mathbf{p} \\ & \frac{\pi^2 U_0^2 \tau \omega p_F}{v_F |q| |\sin \phi|} \langle \mathbf{p} + \mathbf{q}, K' | \mathbf{J}_{K'K'}(\mathbf{p} + \mathbf{q}, \mathbf{p} + \mathbf{q}) | \mathbf{p} + \mathbf{q}, K' \rangle_c \langle \mathbf{p}, K | (\mathbf{u}^* \cdot \boldsymbol{\sigma}) | \mathbf{p} + \mathbf{q}, K' \rangle_c \langle \mathbf{p} + \mathbf{q}, K' | (\mathbf{u} \cdot \boldsymbol{\sigma}) | \mathbf{p}, K \rangle_c \end{aligned}$$

Close to the threshold doping, at the angles ϕ such that $|\sin \phi| \ll \frac{1}{\sqrt{v_F |q| \tau}}$, the divergent factor $1/|\sin \phi|$ has to be replaced by the cutoff $\sqrt{v_F |q| \tau}$ due to the intrinsic scattering processes in graphene.

Drag current at zero temperature

Projecting Eq. (95) on the states of conduction band, be obtain

$$\begin{aligned} \mathbf{j}^{\text{DC}} &= \frac{\pi^2 U_0^2 \tau \omega p_F}{v_F^2 |q| |\sin \phi|} [\langle \mathbf{p}, K | \mathbf{J}_{KK}(\mathbf{p}, \mathbf{p}) | \mathbf{p}, K \rangle_c - \langle \mathbf{p} + \mathbf{q}, K' | \mathbf{J}_{K'K'}(\mathbf{p} + \mathbf{q}, \mathbf{p} + \mathbf{q}) | \mathbf{p} + \mathbf{q}, K' \rangle_c] \times \\ & \langle \mathbf{p}, K | (\mathbf{u}^* \cdot \boldsymbol{\sigma}) | \mathbf{p} + \mathbf{q}, K' \rangle_c \langle \mathbf{p} + \mathbf{q}, K' | (\mathbf{u} \cdot \boldsymbol{\sigma}) | \mathbf{p}, K \rangle_c \end{aligned} \quad (100)$$

Finally, keeping the contribution $\langle J_{KK} \rangle$ only, restoring the factors of \hbar , and expressing the life-time τ through the Drude conductivity of graphene $\rho_g = \frac{\pi \hbar^2}{e^2 \mu \tau}$, where μ denotes the chemical potential, we obtain the dc drag current at zero temperature in the form

$$\mathbf{j}^{\text{DC}} = \frac{\pi^3 U_0^2 (\mathbf{v}_0 \cdot \mathbf{Q})}{e \hbar \rho_g v_F^2 |q|} \frac{\mathbf{F}^{\text{DC}}(\alpha, \phi)}{|\sin \phi|}. \quad (101)$$

BERRY CURVATURE

The emergence of the Hall component of the drag current is analogous to the nonlinear Hall effect explored in Refs. [19, 20]. For a spatially homogeneous periodic electric field, the relationship between the DC drag current and the Berry curvature is given by the formula (the elementary charge is set to 1)

$$\mathbf{j}_a^{\text{DC}} = \epsilon_{adc} \mathcal{E}_b \mathcal{E}_c^* \frac{\tau}{1 + i\omega\tau} \int_{\mathbf{p}} \left(\frac{\partial f_0(\mathbf{p})}{\partial p_b} \right) \Omega_d. \quad (102)$$

For the inter-valley nonlinear Hall effect, Eq. (102) is modified due to additional constraints imposed by momentum and energy conservation requirements in intervalley scattering

$$\mathbf{j}_a^{\text{DC}} = \epsilon_{adc} \mathcal{E}_b \mathcal{E}_c^* \tau \int_{\mathbf{p}} \left(\frac{\partial f_0(\mathbf{p})}{\partial p_b} \right) \delta(|\mathbf{p} + \mathbf{q}| - |\mathbf{p}| - \omega) \Omega_d \approx \epsilon_{adc} \mathcal{E}_b \mathcal{E}_c^* \frac{\tau \omega}{v_F} \int_{\mathbf{p}} \frac{p_b}{p_F} \delta(|\mathbf{p}| - p_F) \delta(|\mathbf{p} + \mathbf{q}| - p_F) \Omega_d \quad (103)$$

where in the last equation we consider the limit $\omega\tau \ll 1$. Here $f_0(\mathbf{p})$ denotes the Fermi distribution, \mathcal{E} denotes the complex-valued amplitude of the electric field, which is related to the periodic electric field by $\mathbf{E} = \mathcal{E} e^{i\omega t}$, and the

indexes a, b, c, d take possible values x, y, z . Ω_d denotes the d -component of the Berry curvature. In a two-dimensional system, the only component of the Berry curvature entering Eq. (102) is Ω_z . In the case of Coulomb drag by a moving polar crystal, the external electric field is determined by the gradient of the potential created by the moving lattice. Transforming the drag Hamiltonian Eq. (46) back to coordinate space, we obtain

$$H_d = \frac{U_0}{2} \int d\mathbf{R} d\mathbf{r} \Psi_{K'}^+(\mathbf{R}) (\mathbf{u}(\mathbf{R}, \mathbf{r}) \cdot \boldsymbol{\sigma}) \Psi_K(\mathbf{R} - \mathbf{r}) e^{-i\omega t} + \text{h.c.} \quad (104)$$

Here the potential $\mathbf{u}(\mathbf{R}, \mathbf{r})$ is given by

$$\mathbf{u}(\mathbf{R}, \mathbf{r}) = e^{i\mathbf{q}\mathbf{R}} \int_{\mathbf{p}} \mathbf{u}(\mathbf{p}, \mathbf{q}) e^{i\mathbf{p}\mathbf{r}}. \quad (105)$$

Explicit expressions for $\mathbf{u}(\mathbf{p}, \mathbf{q})$ as given by Eqs. (47) – (50) show that the components u_0 and u_3 are local, proportional to $\delta(\mathbf{r})$, while the components u_1 and u_2 are short-ranged in \mathbf{r} . Therefore, for the determination of the electric field we consider the potential as completely local and use the definition

$$\mathcal{E}(\mathbf{R}) = -U_0 (\nabla_{\mathbf{R}} \mathbf{u}(\mathbf{R}, \mathbf{r}) \cdot \boldsymbol{\sigma}) = -i\mathbf{q} e^{i\mathbf{q}\mathbf{R}} \int_{\mathbf{p}} (\mathbf{u}(\mathbf{p}, \mathbf{q}) \cdot \boldsymbol{\sigma}) e^{i\mathbf{p}\mathbf{r}} \quad (106)$$

Performing the Fourier transform with respect to \mathbf{R}, \mathbf{r} , we obtain the electric field as

$$\mathcal{E}(\mathbf{p}, \mathbf{q}) = -iU_0 \mathbf{q} (\mathbf{u}(\mathbf{p}, \mathbf{q}) \cdot \boldsymbol{\sigma}). \quad (107)$$

For the electric field pointing in the direction of \mathbf{q} , Eq. (103) relates the Berry curvature to the Hall component to the current, which is perpendicular to \mathbf{q}

$$j_H^{\text{DC}} = |\mathcal{E}_q|^2 \frac{\tau \omega p_F}{v_F q} \frac{\cos \phi}{|\sin \phi|} \Omega_z, \quad (108)$$

where ϕ denotes the angle between \mathbf{p} and \mathbf{q} .

Let us now relate the Berry curvature to the component of the drag current perpendicular to the applied field (the Hall component). Note, that according to Eq. (100), the total drag current can be represented as a difference of the partial currents associated to the valleys K and K' as follows

$$\mathbf{j}^{\text{DC}} = \mathbf{j}_K^{\text{DC}} - \mathbf{j}_{K'}^{\text{DC}}, \quad (109)$$

where the partial currents are determined using Eqs. (96), (97)

$$\mathbf{j}_K^{\text{DC}} = \frac{\pi^2 \tau \omega p_F}{2v_F^2 |q|^3 |\sin \phi|} |\mathcal{E}_q|^2 \{ \mathbf{j}_K(\mathbf{p}) e^{i\phi_{\mathbf{p}}} + \mathbf{j}_K^*(\mathbf{p}) e^{-i\phi_{\mathbf{p}}} \}, \quad (110)$$

$$\mathbf{j}_{K'}^{\text{DC}} = \frac{\pi^2 \tau \omega p_F}{2v_F^2 |q|^3 |\sin \phi|} |\mathcal{E}_q|^2 \{ \mathbf{j}_{K'}(\mathbf{p} + \mathbf{q}) e^{i\phi_{\mathbf{p}+\mathbf{q}}} + \mathbf{j}_{K'}^*(\mathbf{p} + \mathbf{q}) e^{-i\phi_{\mathbf{p}+\mathbf{q}}} \}. \quad (111)$$

Comparing Eqs. (110), (111) with Eq. (108), we relate the Hall component of the matrix element of the partial current to the Berry phase as follows

$$\Omega_z = \frac{\pi^2 \Re [j_H^{\text{DC}} e^{i\phi_{\mathbf{p}}}]}{v_F q^2 \cos \phi} \quad (112)$$

Note, that the angles ϕ and $\phi_{\mathbf{p}}$ are different, namely, ϕ denotes the angle between the vectors \mathbf{p} and \mathbf{q} , whereas $\phi_{\mathbf{p}}$ denotes the direction of \mathbf{p} . The relations between the angles is are given by Eqs. (55), (56). Using Eqs. (55), (56) (see also Fig. 4), one can represent the Hall component of the current as

$$j_H^{\text{DC}} = |\mathcal{E}|^2 \frac{\tau \omega p_F}{v_F q} \cot \phi \left[\Omega_z^K(\mathbf{p}) + \Omega_z^K(-\mathbf{p} - \mathbf{q}) + \Omega_z^{K'}(\mathbf{p} + \mathbf{q}) + \Omega_z^{K'}(-\mathbf{p}) \right]. \quad (113)$$

Therefore, the Hall component of the drag current measures the sum of the Berry phases in K and K' valleys, which we denote as

$$\bar{\Omega}(\mathbf{p}, \mathbf{q}) = \Omega_z^K(\mathbf{p}) + \Omega_z^K(-\mathbf{p} - \mathbf{q}) + \Omega_z^{K'}(\mathbf{p} + \mathbf{q}) + \Omega_z^{K'}(-\mathbf{p}) \quad (114)$$

The sum of the Berry phases Eq. (114) can be calculated from the relation of the longitudinal (with respect to \mathbf{q}) j_q and Hall, j_H components of the drag current

$$\bar{\Omega}(\mathbf{p}, \mathbf{q}) = \frac{\pi^2}{v_F q^2 \cos \phi} \frac{j_H^{\text{DC}}}{j_q^{\text{DC}}} \Re \{ j_{q,K}(\mathbf{p}) e^{i\phi_{\mathbf{p}}} + j_{q,K'}(\mathbf{p} + \mathbf{q}) e^{i\phi_{\mathbf{p}+\mathbf{q}}} \} \quad (115)$$

Here the components of the drag current j_H^{DC} , j_q^{DC} are given by experimental measurements, whereas the matrix elements $j_{q,K}(\mathbf{p})$, $j_{q,K'}(\mathbf{p} + \mathbf{q})$ are calculated by projecting Eqs. (57), (58) on the direction of \mathbf{q} .

ESTIMATIONS OF THE THRESHOLD DOPING LEVEL

To estimate the threshold doping level, we use the following numerical values: the absolute value of the inverse lattice vector of the square ice $Q = \frac{2\pi}{a_0} = \frac{2\pi}{2.8} 10^{10} \text{m}^{-1} \approx 2.24 \cdot 10^{10} \text{m}^{-1}$; the distance between the K and K' points $|\mathbf{K} - \mathbf{K}'| = \frac{4\pi}{3\sqrt{3}a} = \frac{4\pi}{3\sqrt{31.42}} \cdot 10^{10} \text{m}^{-1} \approx 1.7 \cdot 10^{10} \text{m}^{-1}$. The threshold chemical potential corresponds to the Fermi wave vector $p_F \approx q/2$. For the parallel orientation of \mathbf{q} and $\mathbf{K} - \mathbf{K}'$, we obtain $q = Q - |\mathbf{K} - \mathbf{K}'| \approx 0.54 \cdot 10^{10} \text{m}^{-1}$, which corresponds to the Fermi energy $E_F = \hbar v_F q/2 \approx 1.7 \text{eV}$. This value is below the energy of the van Hove singularity at the M-point $E_{vH} \approx 2 \text{eV}$.